metals

MDPI

Article

Prediction of Activity Coefficients and Osmotic Coefficient of Electrolyte Solutions Containing Rb^+ by the Electrolyte Molecular Interaction Volume Model and the Electrolyte Molecular Interaction Volume Model-Energy Term

Yanshan Wu and Dongping Tao *

School of Metallurgy and Energy Engineering, Kunming University of Science and Technology, Kunming 650093, China; yanshan_w@163.com

* Correspondence: dongpingt@aliyun.com; Tel.: +86-15308891226

Abstract: The purpose of this study is to predict two-electrolyte solutions containing Rb^+, explore its characteristics to better solve the problems existing in the natural environment, and promote the development of high technology. We fit and predict the activity and osmotic coefficients of nineteen single-electrolyte solutions and seven two-electrolyte solutions containing Rb^+ using the electrolytr Molecular Interaction Volume Model and the electrolyte Molecular Interaction Volume Model-Energy Termmodels. The average relative errors of the activity coefficient and osmotic coefficient calculated by eMIVM in aqueous monoelectrolyte solution were 0.59% and 0.38%, respectively, and for eMIVM-ET they were 1.06% and 0.38%, respectively. The average relative errors of activity coefficient and osmotic coefficient calculated by eMIVM-ET in organic single-electrolyte solution were 1.33% and 0.48%, respectively, while for eMIVM they were 1.49% and 0.48%, respectively. When predicting the activity coefficient and osmotic coefficient of two-electrolyte solutions containing Rb^+, the average relative errors calculated by the eMIVM-ET model were 23% and 13%, respectively, while the values calculated by the eMIVM model were 34% and 17%, respectively. The results show that eMIVM-ET has a good fitting effect in organic monoelectrolyte solutions, and eMIVM has a good fitting effect in aqueous monoelectrolyte solutions. In the prediction of two-electrolyte solutions, the eMIVM-ET model performs better than the eMIVM model.

Keywords: activity coefficient prediction; osmotic coefficient prediction; electrolyte solutions containing Rb^+; eMIVM; eMIVM-ET

check for updates

Citation: Wu, Y.; Tao, D. Prediction of Activity Coefficients and Osmotic Coefficient of Electrolyte Solutions Containing Rb^+ by the Electrolyte Molecular Interaction Volume Model and the Electrolyte Molecular Interaction Volume Model-Energy Term. *Metals* **2024**, *14*, 245. https://doi.org/10.3390/met14020245

Academic Editors: Ilhwan Park and Denise Crocce Romano Espinosa

Received: 13 January 2024
Revised: 14 February 2024
Accepted: 16 February 2024
Published: 17 February 2024

1. Introduction

The aim of this article, focusing on the prediction of bielectrolyte solutions containing Rb+, is to comprehend the inherent properties of Rb+ electrolyte solutions. This understanding contributes to addressing challenges in the natural environment and facilitating advancements in high technology. With the onset of the world's third industrial revolution, the thermodynamics of electrolyte solutions assumes an increasingly pivotal role across various domains, including chemical engineering [1,2], hydrometallurgy [3–5], environmental biochemistry, salt lake development [6,7], and geochemistry [8–11]. Rubidium metal is significant as an essential rare metal, with Japan and the United States being the primary global consumers. Japan utilizes rubidium as a catalyst for organic synthesis, while the United States predominantly employs it for high-tech development. In our country, rubidium finds applications in the military and scientific sectors and in numerous civilian domains. The use of rubidium ion electrolyte solutions, known for their high conductivity and robust stability, supports the advancement of efficient, long-life energy storage systems [12], including solid-state and hybrid ion batteries. These batteries exhibit substantial potential in electric vehicles and renewable energy storage. Additionally, the application

of their selective permeability and chemical stability aids in developing environmentally friendly membrane separation and wastewater treatment technologies, addressing global challenges of water scarcity and pollution [13]. Consequently, studying the thermodynamic properties of electrolyte solutions containing Rb+ is imperative.

In practical terms, determining activity coefficients and osmotic coefficients is a complex process, typically involving the following [14–16]: (1) experimental methods such as the electric potential method, conductivity method, and permeability method [17]; and (2) theoretical calculation methods based on the chemical properties, state parameters, physicochemical properties, etc., of different substances. The availability of a thermodynamic model capable of more accurately predicting activity and osmotic coefficients would greatly facilitate related research, saving significant time and resources [18]. The theory of ionic mutual attraction, proposed by Debye–Hückel [19–21] in 1923, represents a significant advancement in the theoretical study of modern electrolyte solutions. While effective for Coulombic forces, Debye–Hückel's theory neglects the direct impacts of short-range forces. In response, Pitzer [22–25] introduced considerations for short-range push repulsion between ions, building upon the Debye–Hückel framework [26,27]. However, this approach faces challenges, including the empirical nature of the equation [28], the empirical character of the parameters [29], and an excessive number of parameters [30]. Other models favored by industry for their simplicity and ease of use are the electrolyte nonrandom two-liquid model [31–33], the extended UNIQUAC model [34–36] and the MSE model [37,38], all of which are used to describe the short-range interactions of electrolyte solutions, but which have their corresponding drawbacks. eNRTL equations are inherently poorly grounded in theory. Compared to eNRTL, the extended universal quasichemical model has a more sound theoretical basis, the excess Gibbs energy of the model includes enthalpy and entropy contributions, and the model parameters are ion-specific. However, the model requires four adjustable parameters to describe a single-electrolyte system, including a volume parameter, a surface area parameter and two temperature-dependent binary interaction parameters. The MSE model was developed by Wang et al. (2002) specifically for concentrated electrolyte solutions; the basic model equations also include three components: long-range (LR), mid-range (MR), and short-range interactions (SR), but there is high computational complexity [39]. From these considerations, the Electrolyte Molecular Interaction Volume Model (eMIVM) [40] emerged, aiming to account for both long-range [41] and short-range interactions while utilizing fewer parameters. Within this framework, the eMIVM-ET model [42,43] was proposed within this framework, eliminating the need for ionic molar volume parameters and relying on only two electrolyte-property parameters. The energy terms eMIVM-ET and eMIVM of the electrolyte molecular interaction volume model are thermodynamic models of electrolyte solutions obtained based on sound statistical thermodynamics.

This paper focuses on fitting the activity coefficient and osmotic coefficient of a single-electrolyte solution containing Rb^+ by the eMIVM-ET model and the eMIVM model and predicting the activity coefficient and osmotic coefficient of a three-component system containing a two-electrolyte solution of Rb^+ based on the basic parameters of binary-system data fitting, and finally comparing the computed results to explore the eMIVM-ET and the eMIVM models' applicability.

2. Thermodynamic Modelling Framework

An electrolyte solution system is characterized by the ions and molecules present in the solution, with three types of interactions: ion–ion interactions, ion–molecule interactions, and molecule–molecule interactions. These interactions are the main cause of the thermodynamic properties and phase behavior of the electrolyte solution deviating from the ideal solution, in which the ion–ion interaction can also be called the long-range electrostatic interaction, the potential energy induced by it is inversely proportional to the distance 1/r, and the influence of this kind of interaction has a relatively long range. In addition, ion–molecule interaction and molecule–molecule interaction can be attributed to

the short-range interactions, the potential energy induced by them is inversely proportional to the distance $1/r^6 \sim 1/r^2$, and the influence range of such interactions is relatively short. Therefore, to accurately describe the thermodynamic properties of the electrolyte solution, the model needs to consider the effects of the above interactions. Currently, the main idea of G^{ex} model building is to combine the equations expressing the long-range electrostatic interactions and short-range interactions, i.e., the long-range term and the short-range term, respectively. Robinson and Stokes (1970) state that long-range interactions predominate mainly in low-concentration electrolyte solutions, while short-range interactions predominate in high-concentration electrolyte solutions. The eMIVM model, i.e., MIVM [44], is used to express the short-range interaction term for electrolyte solutions, and the Pitzer–Debye–Hückel model is used to express the long-range electrostatic interaction term. The eMIVM-ET model improves on the eMIVM model by expressing the short-range interaction terms so that the eMIVM-ET model requires only two characterization parameters for a single electrolyte, does not require the ion molar-volume parameter and focuses more on the short-range ion–molecule and molecule–molecule interactions.

Since the MIVM is a symmetric model based on a symmetric reference state, in order to incorporate the PDH equations the MIVM is transformed into an asymmetric reference, i.e., an infinite dilution is used as the reference state. Therefore, the asymmetric molar excess Gibbs free energy of eMIVM is expressed as:

$$G_{\mathrm{m}}^{ex^*,eMIVM} = G_{\mathrm{m}}^{ex^*,PDH} + G_{\mathrm{m}}^{ex^*,MIVM} \tag{1}$$

where the asterisk $*$ represents asymmetry; the excess Moore Gibbs free energy expression for the PDH equation is $G_{\mathrm{m}}^{ex^*,PDH}$; and the excess Moore Gibbs free energy expression for the MIVM equation is $G_{\mathrm{m}}^{ex^*,MIVM}$.

2.1. Long-Range Terms

The excess Moore Gibbs energy expression for the long-range term is given by [41,45]:

$$\frac{G_{\mathrm{m}}^{ex^*,PDH}}{RT} = -(\sum_i x_i)(\frac{1000}{M_S})^{1/2}(\frac{4A_\Phi I_x}{\rho})\ln(1+\rho I_x^{1/2}) \tag{2}$$

where i is the solution component; x_i is the mole fraction of the component; A_Φ is the Debye–Hückel parameter, and at 298.15 K, A_Φ = 0.3915 ($kg^{1/2}\cdot mol^{1/2}$); T is the absolute temperature; M_S is the molecular weight of the solvent; ρ is the ion closest-distance parameter, and Pitzer found that ρ taken as 14.9 gives better calculations; and I_x is the ionic strength in terms of the mole fraction of the ion:

$$I_x = \frac{1}{2}\sum_i z_i^2 x_i \tag{3}$$

The expression for the ionic coefficients of the activity coefficient equation for the PDH long-range term is:

$$\ln\gamma_i^{*,PDH} = -A_\phi(\frac{1000}{M_s})\left[\frac{2z_i^2}{\rho}\ln\left(1+\rho I_x^{\frac{1}{2}}\right) + \frac{z_i^2 I_x^{\frac{1}{2}} - 2I_x^{\frac{3}{2}}}{1+\rho I_x^{\frac{1}{2}}}\right] \tag{4}$$

z_i is the charge number, and for solvent molecules $z_i = 0$ the molecular activity coefficient expression is:

$$\ln\gamma_s^{PDH} = -A_\phi(\frac{1000}{M_s})^{\frac{1}{2}}\frac{2A_\phi I_x^{\frac{3}{2}}}{1+\rho I_x^{\frac{1}{2}}} \tag{5}$$

2.2. eMIVM Short-Range Items

The excess Moore Gibbs energy expression for the eMIVM short-range term is given by [40]:

$$\frac{G_m^{ex,MIVM}}{RT} = -\frac{1}{2}\left[\begin{array}{l} \sum_s Z_s x_s \dfrac{\sum_j x_j B_{js} \ln B_{js}}{\sum_k x_k B_{ks}} \\ +\sum_c Z_c x_c \sum_{a'} \left(\dfrac{x_{a'}}{\sum_{a''} x_{a''}}\right) \dfrac{\sum_j x_j B_{jc,a'c} \ln B_{jc,a'c}}{\sum_k x_k B_{kc,a'c}} \\ +\sum_a Z_a x_a \sum_{c'} \left(\dfrac{x_{c'}}{\sum_{c''} x_{c''}}\right) \dfrac{\sum_j x_j B_{ja,c'a} \ln B_{ja,c'a}}{\sum_k x_k B_{ka,c'a}} \end{array}\right] + \sum_s x_s \ln\left(\frac{V_{ms}}{\sum x_k B_{ks} V_{mk}}\right) \tag{6}$$

where the B parameter is the only adjustable parameter of the model; V_{mi} is the molar volume of the particles ($cm^3 \cdot mol^{-1}$); and Z_i is the coordination number of the particles, when the coordination number is 10. The minimum deviation value can be obtained for most electrolyte systems, so in this study the coordination number of the particles are all taken as 10. j and k represent all the particles, c represents the cations and a represents the anions; as can be seen from Equation (6), the right-hand side of the equation contains an energy term and a volume term. The energy term is used to express the interactions between the particles (enthalpy), and the volume term is used to express the number of microstates of the particles' configurations (entropy).

Based on the relationship between molar and partial-molar quantities at constant temperature and pressure:

$$\begin{aligned} \overline{G}_i^{ex} &= RT \ln \gamma_i = \left[\frac{\partial (nG_m^{ex})}{\partial n_i}\right]_{T,p,n_{j\neq i}} \\ &= G_m^{ex} + \left(\frac{\partial G_m^{ex}}{\partial x_i}\right)_{T,p,x_{k\neq i}} - \sum_{j=1}^{C-1} x_j \left(\frac{\partial G_m^{ex}}{\partial x_j}\right)\left(\frac{\partial G_m^{ex}}{\partial x_i}\right)_{T,p,x_{k\neq j}} \end{aligned} \tag{7}$$

The activity coefficient equations for each particle can be obtained by Equations (6) and (7). For molecules:

$$\ln \gamma_s^{MIVM} = -\frac{1}{2}\left[\begin{array}{l} Z_s \dfrac{\sum_j x_j B_{js} \ln B_{js}}{\sum_k x_k B_{ks}} + \sum_{s'} Z_{s'} \dfrac{x_{s'} B_{ss'}}{\sum_k x_k B_{ks}} \left(\ln B_{ss'} - \dfrac{\sum_k x_k B_{ks'} \ln B_{ks'}}{\sum_k x_k B_{ks'}}\right) \\ +\sum_c Z_c \sum_{a'} \left(\dfrac{x_{a'}}{\sum_{a''} x_{a''}}\right) \dfrac{x_c B_{sc,a'c}}{\sum_k x_k B_{kc,a'c}} \left(\ln B_{sc,a'c} - \dfrac{\sum_k x_k B_{kc,a'c} \ln B_{kc,a'c}}{\sum_k x_k B_{kc,a'c}}\right) \\ +\sum_a Z_a \sum_{c'} \left(\dfrac{x_{c'}}{\sum_{c''} x_{c''}}\right) \dfrac{x_a B_{sa,c'a}}{\sum_k x_k B_{ka,c'a}} \left(\ln B_{sa,c'a} - \dfrac{\sum_k x_k B_{ka,c'a} \ln B_{ka,c'a}}{\sum_k x_k B_{ka,c'a}}\right) \end{array}\right] \\ + \ln\left(\frac{V_{ms}}{\sum_k x_k B_{ks} V_{mk}}\right) + \sum_{s'} x_{s'} \left(1 - \frac{B_{ss'} V_{ms}}{\sum_k x_k B_{ks'} V_{mk}}\right) \end{aligned} \tag{8}$$

For cations:

$$\ln \gamma_c^{MIVM} = -\frac{1}{2}\left[\begin{array}{l} Z_c \sum\limits_{a'} \left(\dfrac{x_{a'}}{\sum\limits_{a''} x_{a''}} \right) \dfrac{\sum\limits_k x_k B_{kc,a'c} \ln B_{kc,a'c}}{\sum\limits_k x_k B_{kc,a'c}} \\ + \sum\limits_s Z_s \dfrac{x_s B_{cs}}{\sum\limits_k x_k B_{ks}} \left(\ln B_{cs} - \dfrac{\sum\limits_k x_k B_{ks} \ln B_{ks}}{\sum\limits_k x_k B_{ks}} \right) \\ + \sum\limits_a Z_a \sum\limits_{c'} \left(\dfrac{x_{c'}}{\sum\limits_{c''} x_{c''}} \right) \dfrac{x_a B_{ca,c'a}}{\sum\limits_k x_k B_{ka,c'a}} \left(\ln B_{ca,c'a} - \dfrac{\sum\limits_k x_k B_{ka,c'a} \ln B_{ka,c'a}}{\sum\limits_k x_k B_{ka,c'a}} \right) \end{array}\right] + \sum\limits_s x_s \left(1 - \frac{B_{cs} V_{mc}}{\sum\limits_k x_k B_{ks} V_{mk}} \right) \tag{9}$$

For anions:

$$\ln \gamma_a^{MIVM} = -\frac{1}{2}\left[\begin{array}{l} Z_a \sum\limits_{a'} \left(\dfrac{x_{c'}}{\sum\limits_{c''} x_{c''}} \right) \dfrac{\sum\limits_k x_k B_{ka,c'a} \ln B_{ka,c'a}}{\sum\limits_k x_k B_{ka,c'a}} \\ + \sum\limits_s Z_s \dfrac{x_s B_{as}}{\sum\limits_k x_k B_{ks}} \left(\ln B_{as} - \dfrac{\sum\limits_k x_k B_{ks} \ln B_{ks}}{\sum\limits_k x_k B_{ks}} \right) \\ + \sum\limits_c Z_c \sum\limits_{a'} \left(\dfrac{x_{a'}}{\sum\limits_{a''} x_{a''}} \right) \dfrac{x_c B_{ac,a'c}}{\sum\limits_k x_k B_{kc,a'c}} \left(\ln B_{ac,a'c} - \dfrac{\sum\limits_k x_k B_{kc,a'c} \ln B_{kc,a'c}}{\sum\limits_k x_k B_{kc,a'c}} \right) \end{array}\right] + \sum\limits_s x_s \left(1 - \frac{B_{as} V_{ma}}{\sum\limits_k x_k B_{ks} V_{mk}} \right) \tag{10}$$

2.3. eMIVM-ET Short-Range Items

The eMIVM-ET model improves on the eMIVM model in that the long-range term of both models is the Pitzer–Debye–Hückel equation, with the main difference being that the expressions for the short-range interactions are different. Compared to eMIVM, eMIVM-ET requires only two characteristic parameters for a single electrolyte and does not require ion molar-volume parameters.

Generalization of the eMIVM-ET [42,43] short-range term:

$$\begin{aligned} g = -\frac{2G_m^{ex}}{RT} &= \sum_{i=1}^{L} Z_{c_i} x_{c_i} \sum_{k=1}^{L} \frac{x_{a_k}}{\sum\limits_{n=1}^{L} x_{a_n}} \left[\frac{\sum\limits_{l=1}^{L} x_{a_l} B_{a_l c_i, a_k c_i} \ln B_{a_l c_i, a_k c_i} + \sum\limits_{j=1}^{J} x_{s_j} B_{s_j c_i, a_k c_i} \ln B_{s_j c_i, a_k c_i}}{\sum\limits_{l=1}^{L} x_{a_l} B_{a_l c_i, a_k c_i} + \sum\limits_{j=1}^{J} x_{s_j} B_{s_j c_i, a_k c_i}} \right] \\ &+ \sum_{i=1}^{L} Z_{a_i} x_{a_i} \sum_{k=1}^{L} \frac{x_{c_k}}{\sum\limits_{n=1}^{L} x_{c_n}} \left[\frac{\sum\limits_{l=1}^{L} x_{c_l} B_{c_l a_i, c_k a_i} \ln B_{c_l a_i, c_k a_i} + \sum\limits_{j=1}^{J} x_{s_j} B_{s_j a_i, c_k a_i} \ln B_{s_j a_i, c_k a_i}}{\sum\limits_{l=1}^{L} x_{c_l} B_{c_l a_i, c_k a_i} + \sum\limits_{j=1}^{J} x_{s_j} B_{s_j a_i, c_k a_i}} \right] \\ &+ \sum_{j=1}^{J} Z_{s_j} x_{s_j} \left[\frac{\sum\limits_{l=1}^{L} \left(x_{c_l} B_{c_l s_j, s_j s_j} \ln B_{c_l s_j, s_j s_j} + x_{a_l} B_{a_l s_j, s_j s_j} \ln B_{a_l s_j, s_j s_j} \right) + \sum\limits_{t=1}^{J} x_{s_t} B_{s_t s_j, s_j s_j} \ln B_{s_t s_j, s_j s_j}}{\sum\limits_{l=1}^{L} x_{c_l} B_{c_i s_j, s_j s_j} + \sum\limits_{l=1}^{L} x_{a_l} B_{a_l s_j, s_j s_j} + \sum\limits_{t=1}^{J} x_{s_t} B_{s_t s_j, s_j s_j}} \right] \end{aligned} \tag{11}$$

In Equation (11) $L = 2$, $J = 1$; B is the binary parameter to be fitted, where B_{ak} and B_{ck} are denoted, respectively, as:

$$B_{ak} = \frac{x_{a_k}}{\sum_{n=1}^{L} x_{a_n}}, B_{ck} = \frac{x_{c_k}}{\sum_{n=1}^{L} x_{c_n}}; \tag{12}$$

$B_{c_l s_j, s_j}$ and $B_{a_l s_j, s_j}$ are denoted as:

$$B_{c_l s_j, s_j} = \frac{\sum_{l=1}^{L} z_{a_l} x_{a_l} B_{ca_l, s_j}}{\sum_{l=1}^{L} z_{a_l} x_{a_l}}, B_{a_l s_j, s_j} = \frac{\sum_{l=1}^{L} z_{c_l} x_{c_l} B_{ac_l, s_j}}{\sum_{l=1}^{L} z_{c_l} x_{c_l}} \tag{13}$$

According to the equation for the relationship between the partial molarity and the molarity [46]:

$$\overline{g}_i = g + \left(\frac{\partial g}{\partial x_i}\right)_{k \neq i, C} - \sum_{j=1}^{C-1} \left(\frac{\partial g}{\partial x_j}\right)_{k \neq i, C} \tag{14}$$

Here, $x_c = 1 - \sum_{j=1}^{C-1} x_j$, $C = 2L + J$, $C = 2L + J$, $C = 5$, $x_{s_1} = 1 - x_{c_1} - x_{c_2} - x_{a_1} - x_{a_2}$ is chosen as the dependent variable.

The expression for the activity coefficient of the short-range term of eMIVM-ET is given below.

For the molecule:

$$\ln \gamma_s^{MIVM} = -\frac{1}{2} \left[\begin{array}{l} \sum_{i=1}^{L} Z_{c_i} x_{c_i} \sum_{k=1}^{L} B_{ak} \left[\frac{\sum_{l=1}^{L} x_{a_l} B_{a_l c_i, a_k c_i} B_{s_J c_i, a_k c_i} \ln \frac{B_{s_J c_i, a_k c_i}}{B_{a_l c_i, a_k c_i}}}{\left(\sum_{l=1}^{L} x_{a_l} B_{a_l c_i, a_k c_i} + x_{S_J} B_{s_J c_i, a_k c_i} \right)^2} \right] \\ + \sum_{i=1}^{L} Z_{a_i} x_{a_i} \sum_{k=1}^{L} B_{ck} \left[\frac{\sum_{l=1}^{L} x_{c_l} B_{c_l a_i, c_k a_i} B_{s_J a_i, c_k a_i} \ln \frac{B_{s_J a_i, c_k a_i}}{B_{c_l a_i, c_k a_i}}}{\left(\sum_{l=1}^{L} x_{c_l} B_{c_l a_i, c_k a_i} + x_{S_J} B_{s_J a_i, c_k a_i} \right)^2} \right] \\ + \sum_{t=1}^{J} Z_{s_J} x_{s_J} \left[\frac{\sum_{l=1}^{L} \left(x_{a_l} B_{a_l s_J, s_J} B_{s_t s_J, s_J} \ln \frac{B_{s_t s_J, s_J}}{B_{a_l s_J, s_J}} + x_{c_l} B_{c_l s_J, s_J} B_{s_t s_J, s_J} \ln \frac{B_{s_t s_J, s_J}}{B_{c_l s_J, s_J}} \right)}{\left(\sum_{l=1}^{L} x_{c_l} B_{c_i s_J, s_J} + \sum_{l=1}^{L} x_{a_l} B_{a_l s_J, s_J} + \sum_{t=1}^{J} x_{s_t} B_{s_t s_J, s_J} \right)^2} \right] \\ + Z_{s_J} \left[\frac{\sum_{l=1}^{L} \left(x_{c_l} B_{c_l s_J, s_J} \ln B_{c_l s_J, s_J} + x_{a_l} B_{a_l s_J, s_J} \ln B_{a_l s_J, s_J} \right) + \sum_{t=1}^{J} x_{s_t} B_{s_t s_J, s_J} \ln B_{s_t s_J, s_J}}{\sum_{l=1}^{L} x_{c_l} B_{c_i s_J, s_J} + \sum_{l=1}^{L} x_{a_l} B_{a_l s_J, s_J} + \sum_{t=1}^{J} x_{s_t} B_{s_t s_J, s_J}} \right] \end{array} \right] \tag{15}$$

For cations:

$$\ln \gamma_c^{MIVM} = -\frac{1}{2}\left[\begin{array}{l} z_c \sum_{k=1}^{L} B_{ak}\left[\dfrac{\sum_{l=1}^{L} x_{a_l} B_{a_l c,a_k c} + x_{s_J} B_{s_J c,a_k c} \ln B_{s_J c,a_k c}}{\sum_{l=1}^{L} x_{a_l} B_{a_l c,a_k c} + x_{s_J} B_{s_J c,a_k c}}\right] \\ + \sum_{i=1}^{L} z_{a_i} x_{a_i}\left[\dfrac{x_{s_J} B_{ca_i,ca_i} B_{s_J a_i,ca_i} \ln \dfrac{B_{ca_i,ca_i}}{B_{s_J a_i,ca_i}}}{\left(x_c B_{ca_i,ca_i} + x_{s_J} B_{s_J a_i,ca_i}\right)^2}\right] \\ + \sum_{t=1}^{J} z_{s_J} x_{s_J}\left[\dfrac{\sum_{l=1}^{J} x_{a_l} B_{a_l s_J,s_J} B_{cs_J,s_J} \ln \dfrac{B_{cs_J,s_J}}{B_{a_l s_J,s_J}} + x_{s_t} B_{cs_J,s_J} B_{s_t s_J,s_J} \ln \dfrac{B_{cs_J,s_J}}{B_{s_t s_J,s_J}}}{\left(x_c B_{cs_J,s_J} + x_{s_t} B_{s_t s_J,s_J} + \sum_{l=1}^{L} x_{a_l} B_{a_l s_J,s_J}\right)^2}\right] \end{array}\right] \tag{16}$$

For anions:

$$\ln \gamma_a^{MIVM} = -\frac{1}{2}\left[\begin{array}{l} z_a \sum_{k=1}^{L} B_{ck}\left[\dfrac{\sum_{l=1}^{L} x_{c_l} B_{c_l a,c_k a} + x_{s_J} B_{s_J a,c_k a} \ln B_{s_J a,c_k a}}{\sum_{l=1}^{L} x_{c_l} B_{c_l a,c_k a} + x_{s_J} B_{s_J a,c_k a}}\right] \\ + \sum_{i=1}^{L} z_{c_i} x_{c_i}\left[\dfrac{x_{s_J} B_{ac_i,ac_i} B_{s_J c_i,ac_i} \ln \dfrac{B_{ac_i,ac_i}}{B_{s_J c_i,ac_i}}}{\left(x_a B_{ac_i,ac_i} + x_{s_J} B_{s_J c_i,ac_i}\right)^2}\right] \\ + \sum_{t=1}^{J} z_{s_J} x_{s_J}\left[\dfrac{\sum_{l=1}^{J} x_{c_l} B_{c_l s_J,s_J} B_{as_J,s_J} \ln \dfrac{B_{as_J,s_J}}{B_{c_l s_J,s_J}} + x_{s_t} B_{as_J,s_J} B_{s_t s_J,s_J} \ln \dfrac{B_{as_J,s_J}}{B_{s_t s_J,s_J}}}{\left(x_a B_{as_J,s_J} + x_{s_t} B_{s_t s_J,s_J} + \sum_{l=1}^{L} x_{c_l} B_{c_l s_J,s_J}\right)^2}\right] \end{array}\right] \tag{17}$$

The binary expansion of the eMIVM-ET model has two adjustable parameters, $B_{ca,s}$ and $B_{s,ca}$, and has the following relationship:

$$B_{as} = B_{cs} = B_{ca,s} \tag{18}$$

$$B_{sa,ca} = B_{sc,ac} = B_{s,ca} \tag{19}$$

An expression for the average ionic activity coefficient of the electrolyte:

$$\ln \gamma_{\pm}^{*} = \frac{1}{\nu}(\nu_c \ln \gamma_c^{*} + \nu_a \ln \gamma_a^{*}) \tag{20}$$

In Equation (20), $\gamma_{\pm}^{*}$ is the average activity coefficient in units of mole fraction; v_c represents the number of cations in the electrolyte, v_a represents the number of anions in the electrolyte, and $v = v_a + v_c$. Since most of the experimental data are in units of mass molar concentration, a transformation of Equation (20) is required to transform the average ion activity coefficient $\gamma_{\pm x}^{*}$ in units of mole fraction to the average ion activity coefficient $\gamma_{\pm m}^{*}$ in units of mass molar concentration:

$$\ln \gamma_{\pm m}^{*} = \ln \gamma_{\pm x}^{*} - \ln(1 + 0.001 M_s \sum_i m_i) \tag{21}$$

In addition, the expression for the osmotic coefficient of the multicomponent system is given by:

$$\Phi = -\left(\frac{1000}{M_s \sum_i m_i}\right) \ln(x_s \gamma_s) \tag{22}$$

2.4. Radii and Molar Volumes of Ions in Aqueous Solution

The molar volume of ions can be calculated by the following equation [47]:

$$V_{mi} = \left(\frac{4\pi N_A}{3}\right) r_i^3 = 2522.5 r_i^3 \tag{23}$$

where N_A is Avogadro's constant; r_i (nm) is the radius of the ion in aqueous solution, and the value of r_i (nm) is independent of temperature. Its values are listed in Table 1.

Table 1. The radius and molar volume of ions.

Ion Name	Ionic Radius (mm)	Ionic Molar Volume	Ion Name	Ionic Radius (mm)	Ionic Molar Volume
H^+ [48]	0.030	0.0681	SO_4^{2-} [48]	0.230	30.6913
Na^+ [48]	0.102	2.6769	NO^{2-} [48]	0.192	17.8500
Ag^+ [48]	0.115	3.8400	NO^{3-} [48]	0.179	14.4700
Au^{3+} [48]	0.085	1.5491	AC^- [48]	0.232	31.4989
Tl^+ [49]	0.150	8.5134	ClO_4^- [48]	0.240	34.8700
Ga^{3+} [49]	0.062	0.6012	$S_2O_8^{2-}$ [50]	0.300	68.1075
Au^+ [49]	0.137	0.6012	ReO_4^- [48]	0.280	55.3739
Sc^{3+} [49]	0.073	0.9813	I^- [49]	0.220	26.8596
In^{3+} [49]	0.088	0.7190	Cl^- [50]	0.181	14.9577
Rb^+ [50]	0.149	8.3443	F^- [48]	0.133	5.9345
Cd^{2+} [50]	0.095	2.1627	Br^- [48]	0.196	18.9933

3. Results and Comparison

3.1. Activity-Coefficient Fitting

The binary parameters fitted to the activity coefficient calculations and the deviations and relative errors of the activity coefficient calculations for eMIVM-ET and eMIVM in aqueous solutions containing monoelectrolytes of Rb^+ and organic solutions containing monoelectrolytes of Rb^+ are presented in Tables 2–8.

The binary parameters for aqueous monoelectrolyte solutions containing Rb+, fitted by both the eMIVM-ET and eMIVM models, are presented in Tables 2–4. Specifically, Tables 2 and 3 display the binary parameters fitted by the eMIVM-ET and eMIVM models in aqueous solutions of single electrolytes containing Rb^+ at various temperatures and concentrations. In addition, Table 4 provides the binary parameters fitted by both models in organic solutions of monoelectrolytes containing Rb^+.

Table 2. B parameters fitted by eMIVM-ET and eMIVM activity coefficient at different temperatures (aqueous electrolyte solution).

System	T/K	eMIVM-ET		eMIVM	
		$B_{ca,s}$	$B_{s,ca}$	$B_{ca,s}$	$B_{s,ca}$
RbCl + H_2O [51]	283.15	1.9176	0.2870	2.5368	0.1546
RbCl + H_2O [51]	298.15	1.9505	0.2718	2.5171	0.1558
RbCl + H_2O [51]	313.15	1.9532	0.2706	2.8119	0.1222
RbCl + H_2O [51]	328.15	1.9606	0.2672	2.5571	0.1503
RbCl + H_2O [51]	343.15	1.9678	0.2640	2.5936	0.1457
Rb_2SO_4 + H_2O [52]	298.15	2.1411	0.1973	2.2380	0.1674
Rb_2SO_4 + H_2O [52]	323.15	2.0848	0.2184	2.2402	0.1711

Table 3. B parameters fitted by eMIVM-ET and eMIVM activity coefficient at 298.15 T (aqueous electrolyte solution of different concentrations).

System	eMIVM-ET		eMIVM		m-mol·kg^{-1}
	$B_{ca,s}$	$B_{s,ca}$	$B_{ca,s}$	$B_{s,ca}$	
RbCl + H_2O [53]	0.2024	1.3813	2.2381	0.1988	0.0001–7.8
RbCl + H_2O [53]	2.0179	0.2426	3.4190	0.0830	0.0001–0.1
RbCl + H_2O [53]	1.5475	0.5157	2.2381	0.1988	0.1–7.8
RbF + H_2O [53]	1.7581	0.4049	2.2347	0.2258	0.001–3.5
RbF + H_2O [53]	1.6892	0.4124	3.5520	0.0804	0.001–0.1
RbF + H_2O [53]	1.7560	0.4082	2.2343	0.2259	0.1–3.5
RbBr + H_2O [53]	0.1771	1.3503	2.1714	0.2085	0.0001–5
RbBr + H_2O [53]	2.0273	0.2387	3.3755	0.0842	0.0001–0.1
RbBr + H_2O [53]	0.1815	1.3576	2.1713	0.2085	0.1–5
RbI + H_2O [53]	0.1780	1.3523	2.1358	0.2087	0.0001–5
RbI + H_2O [53]	2.0220	0.2408	3.2895	0.0869	0.0001–0.1
RbI + H_2O [53]	0.1838	1.3618	2.1356	0.2088	0.1–5
$RbNO_2$ + H_2O [54]	2.0351	0.2395	2.1500	0.1992	0.1–7
$RbNO_3$ + H_2O [53]	2.1925	0.1784	1.9814	0.2145	0.001–4.5
$RbNO_3$ + H_2O [53]	2.2047	0.1750	3.6434	0.0698	0.001–0.1
$RbNO_3$ + H_2O [53]	2.1944	0.1772	1.9810	0.2146	0.1–4.5
$RbC_2H_3O_2$ + H_2O [55]	0.4716	1.8612	2.3478	0.1938	0.1–3.5
Rb_2SO_4 + H_2O [55]	2.1153	0.2043	1.8958	0.2491	0.1–1.8
$Rb_2S_2O_8$ + H_2O [56]	2.3887	0.1252	4.5748	0.0358	0.001–0.075

Table 4. B parameters fitted by eMIVM-ET and eMIVM activity coefficient at 298.15 T (organic electrolyte solution).

System	eMIVM-ET		eMIVM	
	$B_{ca,s}$	$B_{s,ca}$	$B_{ca,s}$	$B_{s,ca}$
RbCl-10%DMA-H_2O [57]	0.7356	1.3457	2.1518	0.2054
RbCl-20%DMA-H_2O [57]	0.8436	1.4786	0.7435	0.6284
RbCl-30%DMA-H_2O [57]	2.1461	0.1947	2.2191	0.1789
RbCl-10%DMF-H_2O [58]	2.0141	0.2442	2.0864	0.2230
RbCl-20%DMF-H_2O [58]	2.0688	0.2228	2.2924	0.1768
RbCl-30%DMF-H_2O [58]	2.1475	0.1947	2.5583	0.1349
RbCl-40%DMF-H_2O [58]	2.2454	0.1638	3.0963	0.0883
RbCl-10%EC-H_2O [58]	2.0065	0.2457	1.6307	0.3834
RbCl-20%EC-H_2O [58]	2.1170	0.2028	1.3223	0.4768
RbCl-30%EC-H_2O [58]	2.2278	0.1674	2.0983	0.1848
RbCl-40%EC-H_2O [58]	2.2857	0.1510	2.1443	0.1665
RbCl-10%EG-H_2O [59]	2.0524	0.2293	2.4572	0.1552
RbCl-20%EG-H_2O [59]	2.1277	0.2015	2.5862	0.1343
RbCl-30%EG-H_2O [59]	2.1859	0.1819	2.6739	0.1214
RbCl-40%EG-H_2O [59]	2.2330	0.1678	2.8590	0.1032
RbCl-10%Glycerol-H_2O [60]	1.9786	0.2601	2.5056	0.1527
RbCl-20%Glycerol-H_2O [60]	2.0198	0.2432	2.7230	0.1254
RbCl-30%Glycerol-H_2O [60]	2.0456	0.2331	2.7778	0.1192
RbCl-40%Glycerol-H_2O [60]	2.0824	0.2192	2.9085	0.1065
RbF-10%EG-H_2O [61]	1.7084	0.4010	2.7383	0.1360
RbF-20%EG-H_2O [61]	1.9591	0.2692	3.1232	0.0985
RbF-30%EG-H_2O [61]	2.0748	0.2204	2.5197	0.1497
RbF-40%EG-H_2O [61]	2.1222	0.2034	2.6615	0.1301
RbCl-5%MeOH-5%EtOH-90%H_2O [62]	2.1200	0.2042	2.6436	0.1294
RbCl-10%MeOH-5%EtOH-85%H_2O [62]	2.1559	0.1920	2.7120	0.1201
RbCl-5%MeOH-10%EtOH-85%H_2O [62]	2.1651	0.1888	2.7092	0.1198
RbCl-10%MeOH-10%EtOH-80%H_2O [62]	2.2187	0.1717	2.7664	0.1114
RbCl-15%MeOH-15%EtOH-70%H_2O [62]	2.2854	0.1527	2.8147	0.1025

Table 4. *Cont.*

System	eMIVM-ET		eMIVM	
	$B_{ca,s}$	$B_{s,ca}$	$B_{ca,s}$	$B_{s,ca}$
RbCl-10%TMU-H_2O [63]	0.4986	1.9717	2.8628	0.1208
RbCl-20%TMU-H_2O [63]	0.5660	2.1894	3.0449	0.1034
RbCl-30%TMU-H_2O [63]	0.5532	2.1619	3.0711	0.0997
RbF-10%Glycine-H_2O [62]	1.7922	0.3815	2.0251	0.2998
RbF-20%Glycine-H_2O [62]	1.8403	0.3650	2.0972	0.2925
RbF-30%Glycine-H_2O [62]	1.8572	0.3591	2.1387	0.2840
RbF-40%Glycine-H_2O [62]	0.5815	2.2265	2.1919	0.2771
RbCl-10%methanol-H_2O [64]	2.1409	0.1981	2.3001	0.1646
RbCl-20%methanol-H_2O [64]	2.2745	0.1555	2.3234	0.1451
RbCl-30%methanol-H_2O [64]	2.3759	0.1305	2.4132	0.1218
RbCl-40%methanol-H_2O [64]	2.4833	0.1081	2.9623	0.0757

Note: DMA (dimethylacetamide); DMF (dimethylformamide); EC (ethylene carbonate); EG (ethylene glycol); MeOH (methanol); EtOH (methanol); TMU (tetramethylurea).

Observing Table 2, it is evident that the disparity between the binary parameters fitted for the same system at different temperatures is minimal. This suggests that temperature has a negligible impact on the binary parameters fitted by both models. Observing Table 3, it can be seen that the pattern presented for the same system is that Bca,s is greater in the low-concentration solution than in the high-concentration solution, and Bs,ca is greater in the high-concentration solution than in the low-concentration solution.

Table 5. Deviations and relative errors of eMIVM-ET and eMIVM activity-coefficient fitting at 298.15 T (aqueous electrolyte solution).

System	eMIVM-ET SD	eMIVM SD	eMIVM-ET ARD/%	eMIVM ARD/%
RbF + H_2O [53]	0.0083	0.0017	0.94	0.19
RbCl + H_2O [53]	0.0086	0.0016	1.07	0.18
RbBr + H_2O [53]	0.0063	0.0021	0.77	0.24
RbI + H_2O [53]	0.0082	0.0023	1.02	0.27
$RbNO_2$ + H_2O [53]	0.0103	0.0122	1.54	2.11
$RbNO_3$ + H_2O [53]	0.0100	0.0041	2.07	0.69
$RbC_2H_3O_2$ + H_2O [55]	0.0143	0.0072	1.32	0.71
Rb_2SO_4 + H_2O [55]	0.0010	0.0024	0.36	0.67
$Rb_2S_2O_8$ + H_2O [56]	0.0031	0.0017	0.40	0.24
Average	0.0078	0.0039	1.06	0.59

Note: $SD = \sqrt{\frac{\sum(\gamma_{pre}-\gamma_{exp})^2}{N}}$, $ARD = \frac{1}{N}\sum\left|\frac{\gamma_{pre}-\gamma_{exp}}{\gamma_{exp}}\right| \times 100\%$. γ_{pre} is the calculated value of the activity coefficient; γ_{exp} is the experimental value of the activity coefficient.

Table 6. Deviations and relative errors of eMIVM-ET and eMIVM activity-coefficient fitting at different temperatures (aqueous electrolyte solution).

System	T/K	eMIVM-ET SD	eMIVM SD	eMIVM-ET ARD/%	eMIVM ARD/%
RbCl + H_2O [51]	283.15	0.0025	0.0022	0.17	0.11
RbCl + H_2O [51]	298.15	0.0011	0.0007	0.11	0.07
RbCl + H_2O [51]	313.15	0.0013	0.0007	0.13	0.07
RbCl + H_2O [51]	328.15	0.0012	0.0007	0.14	0.07
RbCl + H_2O [51]	343.15	0.0014	0.0007	0.15	0.07
Rb_2SO_4 + H_2O [52]	298.15	0.0055	0.0041	1.15	0.68
Rb_2SO_4 + H_2O [52]	323.15	0.0089	0.0037	2.26	0.67
Average		0.0031	0.0018	0.59	0.25

Table 7. Deviations and relative errors of eMIVM-ET and eMIVM activity-coefficient fitting at different concentrations at 298.15 T (aqueous electrolyte solution).

System	eMIVM-ET SD	eMIVM SD	eMIVM-ET ARD/%	eMIVM ARD/%	m-mol·kg^{-1}
RbCl + H_2O [53]	0.0004	0.0002	0.04	0.02	0.0001–0.1
RbCl + H_2O [53]	0.0245	0.0016	3.43	0.19	0.1–7.8
RbF + H_2O [53]	0.0020	0.0002	0.18	0.02	0.001–0.1
RbF + H_2O [53]	0.0073	0.0018	0.86	0.22	0.1–3.5
RbBr + H_2O [53]	0.0004	0.0002	0.04	0.02	0.0001–0.1
RbBr + H_2O [53]	0.0033	0.0022	0.45	0.26	0.1–5
RbI + H_2O [53]	0.0004	0.0002	0.04	0.02	0.0001–0.1
RbI + H_2O [53]	0.0046	0.0024	0.63	0.30	0.1–5
$RbNO_3$ + H_2O [53]	0.0008	0.0004	0.08	0.04	0.001–0.1
$RbNO_3$ + H_2O [53]	0.0104	0.0044	2.29	0.81	0.1–4.5
Average	0.0054	0.0014	0.80	0.19	

Table 8. Deviations and relative errors of eMIVM-ET and eMIVM activity-coefficient fitting at 298.15 T (organic electrolyte solution).

System	eMIVM-ET SD	eMIVM SD	eMIVM-ET ARD/%	eMIVM ARD/%
RbCl-10%DMA-H_2O [57]	0.0014	0.0036	0.18	0.35
RbCl-20%DMA-H_2O [57]	0.0046	0.0056	0.63	0.50
RbCl-30%DMA-H_2O [57]	0.0027	0.0073	0.35	0.65
RbCl-10%DMF-H_2O [58]	0.0013	0.0014	0.16	0.18
RbCl-20%DMF-H_2O [58]	0.0033	0.0045	0.40	0.50
RbCl-30%DMF-H_2O [58]	0.0083	0.0092	1.05	1.16
RbCl-40%DMF-H_2O [58]	0.0118	0.0133	1.47	1.65
RbCl-10%EC-H_2O [58]	0.0077	0.0123	0.93	1.75
RbCl-20%EC-H_2O [58]	0.0091	0.0083	1.26	1.25
RbCl-30%EC-H_2O [58]	0.0049	0.0025	0.79	0.54
RbCl-40%EC-H_2O [58]	0.0064	0.0053	1.47	0.85
RbCl-10%EG-H_2O [60]	0.0039	0.0068	0.42	0.82
RbCl-20%EG-H_2O [60]	0.0041	0.0085	0.43	0.99
RbCl-30%EG-H_2O [60]	0.0058	0.0117	0.60	1.37
RbCl-40%EG-H_2O [60]	0.0077	0.0178	0.86	2.18
RbCl-10%Glycerol-H_2O [60]	0.0071	0.0067	0.82	0.80
RbCl-20%Glycerol-H_2O [60]	0.0121	0.0119	1.40	1.44
RbCl-30%Glycerol-H_2O [60]	0.0129	0.0153	1.42	1.82
RbCl-40%Glycerol-H_2O [60]	0.0162	0.0196	1.84	2.39
RbF-10%EG-H_2O [61]	0.0009	0.0031	0.08	0.34
RbF-20%EG-H_2O [61]	0.0042	0.0111	0.41	1.27
RbF-30%EG-H_2O [61]	0.0020	0.0060	0.24	0.67
RbF-40%EG-H_2O [61]	0.0045	0.0135	0.57	1.53
RbCl-5%MeOH-5%EtOH-90%H_2O [62]	0.0072	0.0096	0.62	1.03
RbCl-10%MeOH-5%EtOH-85%H_2O [62]	0.0103	0.0136	0.90	1.61
RbCl-5%MeOH-10%EtOH-85%H_2O [62]	0.0141	0.0143	1.32	1.49
RbCl-10%MeOH-10%EtOH-80%H_2O [62]	0.0069	0.0139	0.76	1.66
RbCl-15%MeOH-15%EtOH-70%H_2O [62]	0.0090	0.0189	0.97	2.33

Table 8. *Cont.*

System	eMIVM-ET SD	eMIVM SD	eMIVM-ET ARD/%	eMIVM ARD/%
RbCl-10%TMU-H_2O [63]	0.0308	0.0111	3.25	1.21
RbCl-20%TMU-H_2O [63]	0.0593	0.0221	6.05	2.35
RbCl-30%TMU-H_2O [63]	0.0641	0.0350	7.04	3.85
RbF-10%Glycine-H_2O [62]	0.0015	0.0042	0.17	0.50
RbF-20%Glycine-H_2O [62]	0.0045	0.0101	0.47	1.17
RbF-30%Glycine-H_2O [62]	0.0079	0.0146	0.83	1.64
RbF-40%Glycine-H_2O [62]	0.0093	0.0170	0.95	1.89
RbCl-10%methanol-H_2O [64]	0.0098	0.0124	1.18	1.85
RbCl-20%methanol-H_2O [64]	0.0087	0.0174	1.37	2.73
RbCl-30%methanol-H_2O [64]	0.0036	0.0194	1.42	3.32
RbCl-40%methanol-H_2O [64]	0.0382	0.0275	6.78	4.62
Average	0.0110	0.0120	1.33	1.49

The deviations and relative errors calculated for the eMIVM-ET and eMIVM models in aqueous-monoelectrolyte versus organic-monoelectrolyte solutions containing Rb^+ are given in Tables 5–8. From the results of the deviations and relative errors, it can be seen that (1) the effect of temperature on the activity coefficient is not significant at different temperatures for the same system; (2) lower-concentration solutions exhibit more minor average deviations and average relative errors within the same system than higher-concentration solutions. In other words, a lower concentration corresponds to a more accurate fitting effect; (3) in aqueous electrolyte solutions, the eMIVM model outperforms the eMIVM-ET model, demonstrating superior accuracy in calculating the average bias and relative error of activity coefficients; and (4) in organic electrolyte solutions, the eMIVM-ET model is slightly better than the eMIVM at calculating the activity coefficients' average bias and relative error. In aqueous single-electrolyte solutions, both the eMIVM-ET model and the eMIVM model calculate the bias of the activity coefficient. The eMIVM model yields deviations of 0.0078 and 0.0039 with relative errors of 1.06% and 0.59%, respectively. In organic electrolyte solutions, the eMIVM-ET and eMIVM models produce deviations of 0.0011 and 0.0012 with relative errors of 1.33% and 1.49%, respectively. In summary, the eMIVM model is applicable to aqueous monoelectrolyte solutions containing Rb^+, and the eMIVM-ET model is applicable to organic monoelectrolyte solutions containing Rb^+.

3.2. Osmotic-Coefficient Fitting

The binary parameters fitted in the osmotic-coefficient calculations and the deviations and relative errors of the osmotic-coefficient calculations for eMIVM-ET and eMIVM in aqueous and organic solutions containing Rb^+ monoelectrolytes and monoelectrolytes, respectively, are presented in Tables 9–13.

The binary parameters fitted by the eMIVM-ET and eMIVM models in aqueous monoelectrolyte solutions containing Rb^+ are given in Table 9. Table 10 gives the binary parameters fitted by the eMIVM-ET and eMIVM models in organic solutions of a single electrolyte containing Rb^+. Table 9 gives the binary parameters fitted by the eMIVM-ET and eMIVM models in aqueous solutions of single electrolytes containing Rb^+ at different concentrations.

The deviations and relative errors calculated for the eMIVM-ET and eMIVM models in aqueous monoelectrolyte solutions containing Rb^+ versus organic monoelectrolyte solutions are given in Tables 11–13. The results of bias and relative error show that (1) for the same system, the average bias and average relative error are more negligible in the low-concentration solution than in the high-concentration solution. That is, the lower the concentration, the better the fitting effect; (2) in aqueous electrolyte solutions, the eMIVM model is slightly better than eMIVM-ET in its ability to calculate the mean deviation and relative error of the osmotic coefficients; and (3) in organic electrolyte solutions, the eMIVM-

ET model is slightly better than eMIVM in its ability to calculate the mean deviation and relative error of the osmotic coefficients. In aqueous monoelectrolyte solutions, the eMIVM-ET model and the eMIVM model calculated deviations of 0.0039 and 0.0038, with relative errors of 0.38% and 0.38%, respectively. In organic electrolyte solutions, the eMIVM-ET and eMIVM models calculated deviations of 0.0047 and 0.0048, with relative errors of 0.48% and 0.48%, respectively, which were minimal differences. In summary, the eMIVM model is applicable to aqueous monoelectrolyte solutions containing Rb^+, and the eMIVM-ET model is applicable to organic monoelectrolyte solutions containing Rb^+.

Table 9. B parameters fitted by eMIVM-ET and eMIVM osmotic coefficient at 298.15 T (aqueous electrolyte solution of different concentrations).

System	eMIVM-ET		eMIVM		m-mol·kg^{-1}
	$B_{ca,s}$	$B_{s,ca}$	$B_{ca,s}$	$B_{s,ca}$	
RbCl + H_2O [53]	2.2939	0.1923	2.2341	0.2000	0.0001–7.8
RbCl + H_2O [53]	3.4583	0.0826	3.3332	0.0874	0.0001–0.1
RbCl + H_2O [53]	2.2939	0.1923	2.2341	0.2000	0.1–7.8
RbF + H_2O [53]	2.2101	0.2311	2.2279	0.2278	0.001–3.5
RbF + H_2O [53]	3.3213	0.0929	3.4588	0.0849	0.001–0.1
RbF + H_2O [53]	2.2098	0.2312	2.2276	0.2278	0.1–3.5
RbBr + H_2O [53]	2.2414	0.2018	2.1542	0.2130	0.0001–5
RbBr + H_2O [53]	2.1954	0.2067	2.0092	0.2406	0.0001–0.1
RbBr + H_2O [53]	2.2413	0.2018	2.1541	0.2130	0.1–5
RbI + H_2O [53]	2.2625	0.1973	2.1163	0.2138	0.0001–5
RbI + H_2O [53]	3.3268	0.0893	3.1250	0.0963	0.0001–0.1
RbI + H_2O [53]	2.2623	0.1973	2.1162	0.2138	0.1–5
$RbNO_2$ + H_2O [54]	2.1551	0.2079	2.0808	0.2177	0.1–7
$RbNO_3$ + H_2O [53]	1.9492	0.2255	1.9195	0.2292	0.001–4.5
$RbNO_3$ + H_2O [53]	3.3983	0.0811	3.3300	0.0828	0.001–0.1
$RbNO_3$ + H_2O [53]	1.9489	0.2256	1.9192	0.2293	0.1–4.5
$RbC_2H_3O_2$ + H_2O [55]	2.5781	0.1675	2.3874	0.1845	0.1–3.5
Rb_2SO_4 + H_2O [55]	2.1269	0.2019	2.0199	0.2150	0.1–1.8
$Rb_2S_2O_8$ + H_2O [56]	4.6858	0.0382	4.3931	0.0388	0.001–0.075

Table 10. B parameters fitted by eMIVM-ET and eMIVM osmotic coefficient at 298.15 T (organic electrolyte solution).

System	eMIVM-ET		eMIVM	
	$B_{ca,s}$	$B_{s,ca}$	$B_{ca,s}$	$B_{s,ca}$
RbCl-10%DMA-H_2O [57]	2.0031	0.2418	0.3490	0.6435
RbCl-20%DMA-H_2O [57]	0.9032	0.5049	1.3194	0.4873
RbCl-30%DMA-H_2O [57]	0.4470	0.4084	1.8483	0.2509
RbCl-10%DMF-H_2O [58]	2.1508	0.2128	2.1031	0.2192
RbCl-20%DMF-H_2O [58]	2.2322	0.1911	2.1868	0.1958
RbCl-30%DMF-H_2O [58]	2.4593	0.1505	2.4142	0.1532
RbCl-40%DMF-H_2O [58]	2.8749	0.1053	2.8279	0.1066
RbCl-10%EC-H_2O [58]	1.6648	0.3620	1.6281	0.3771
RbCl-20%EC-H_2O [58]	1.8270	0.2706	1.7965	0.2764
RbCl-30%EC-H_2O [58]	2.1648	0.1769	2.1279	0.1797
RbCl-40%EC-H_2O [58]	2.1288	0.1722	2.0948	0.1744
RbCl-10%EG-H_2O [60]	2.1476	0.2100	2.0985	0.2165
RbCl-20%EG-H_2O [60]	2.3433	0.1679	2.2985	0.1713
RbCl-30%EG-H_2O [60]	2.3883	0.1552	2.3453	0.1578
RbCl-40%EG-H_2O [60]	2.4896	0.1387	2.4468	0.1407

Table 10. *Cont.*

System	eMIVM-ET		eMIVM	
	$B_{ca,s}$	$B_{s,ca}$	$B_{ca,s}$	$B_{s,ca}$
RbCl-10%Glycerol-H_2O [60]	2.3376	0.1829	2.2867	0.1880
RbCl-20%Glycerol-H_2O [60]	2.5016	0.1561	2.4513	0.1597
RbCl-30%Glycerol-H_2O [60]	2.4451	0.1627	2.3955	0.1666
RbCl-40%Glycerol-H_2O [60]	2.5713	0.1445	2.5220	0.1474
RbF-10%EG-H_2O [61]	1.9811	0.2809	1.9087	0.3105
RbF-20%EG-H_2O [61]	2.5956	0.1484	2.5885	0.1493
RbF-30%EG-H_2O [61]	1.4374	0.4217	1.0942	0.3919
RbF-40%EG-H_2O [61]	1.3732	0.2868	1.3683	0.2859
RbCl-5%MeOH-5%EtOH-90%H_2O [62]	2.3890	0.1631	2.3433	0.1664
RbCl-10%MeOH-5%EtOH-85%H_2O [62]	2.2996	0.1715	2.2558	0.1749
RbCl-5%MeOH-10%EtOH-85%H_2O [62]	2.3358	0.1651	2.2922	0.1682
RbCl-10%MeOH-10%EtOH-80%H_2O [62]	2.3984	0.1501	2.3563	0.1525
RbCl-15%MeOH-15%EtOH-70%H_2O [62]	2.4178	0.1396	2.3780	0.1413
RbF-10%Glycine-H_2O [62]	1.9760	0.3101	2.0101	0.2999
RbF-20%Glycine-H_2O [62]	2.0844	0.2815	2.0536	0.2960
RbF-30%Glycine-H_2O [62]	2.0558	0.2937	2.0599	0.2951
RbF-40%Glycine-H_2O [62]	2.1007	0.2869	2.0966	0.2911

Table 11. Deviations and relative errors of eMIVM-ET and eMIVM osmotic coefficient fitting at 298.15 T (aqueous electrolyte solution).

System	eMIVM-ET SD	eMIVM SD	eMIVM-ET ARD/%	eMIVM ARD/%
RbF + H_2O [53]	0.0021	0.0021	0.16	0.16
RbCl + H_2O [53]	0.0019	0.0014	0.17	0.13
RbBr + H_2O [53]	0.0012	0.0011	0.11	0.10
RbI + H_2O [53]	0.0011	0.0013	0.10	0.11
$RbNO_2$ + H_2O [54]	0.0111	0.0115	1.19	1.23
$RbNO_3$ + H_2O [53]	0.0043	0.0043	0.49	0.49
$RbC_2H_3O_2$ + H_2O [55]	0.0055	0.0051	0.47	0.44
Rb_2SO_4 + H_2O [55]	0.0044	0.0044	0.52	0.51
$Rb_2S_2O_8$ + H_2O [56]	0.0031	0.0030	0.22	0.22
Average	0.0039	0.0038	0.38	0.38

Table 12. Deviations and relative errors of eMIVM-ET and eMIVM osmotic coefficient fitting at 298.15 T (aqueous electrolyte solution of different concentrations).

System	eMIVM-ET SD	eMIVM SD	eMIVM-ET ARD/%	eMIVM ARD/%	m-mol·kg^{-1}
RbCl + H_2O [53]	0.0002	0.0001	0.01	0.01	0.0001–0.1
RbCl + H_2O [53]	0.0020	0.0015	0.19	0.14	0.1–7.8
RbF + H_2O [53]	0.0002	0.0003	0.02	0.02	0.001–0.1
RbF + H_2O [53]	0.0024	0.0024	0.19	0.19	0.1–3.5
RbBr + H_2O [53]	0.0021	0.0021	0.09	0.09	0.0001–0.1
RbBr + H_2O [53]	0.0013	0.0012	0.12	0.11	0.1–5
RbI + H_2O [53]	0.0001	0.0001	0.01	0.01	0.0001–0.1
RbI + H_2O [53]	0.0014	0.0014	0.12	0.12	0.1–5
$RbNO_3$ + H_2O [53]	0.0003	0.0002	0.02	0.02	0.001–0.1
$RbNO_3$ + H_2O [53]	0.0048	0.0048	0.59	0.60	0.1–4.5
Average	0.0015	0.0014	0.14	0.13	-

Table 13. Deviations and relative errors of eMIVM-ET and eMIVM osmotic coefficient fitting at 298.15 T (organic electrolyte solution).

System	eMIVM-ET SD	eMIVM SD	eMIVM-ET ARD/%	eMIVM ARD/%
RbCl-10%DMA-H_2O [57]	0.0012	0.0012	0.12	0.12
RbCl-20%DMA-H_2O [57]	0.0024	0.0050	0.24	0.48
RbCl-30%DMA-H_2O [57]	0.0028	0.0028	0.30	0.30
RbCl-10%DMF-H_2O [58]	0.0016	0.0016	0.15	0.15
RbCl-20%DMF-H_2O [58]	0.0015	0.0015	0.14	0.14
RbCl-30%DMF-H_2O [58]	0.0039	0.0039	0.38	0.38
RbCl-40%DMF-H_2O [58]	0.0066	0.0066	0.70	0.70
RbCl-10%EC-H_2O [58]	0.0080	0.0081	0.83	0.83
RbCl-20%EC-H_2O [58]	0.0079	0.0079	0.90	0.90
RbCl-30%EC-H_2O [58]	0.0057	0.0056	0.70	0.69
RbCl-40%EC-H_2O [58]	0.0039	0.0039	0.45	0.45
RbCl-10%EG-H_2O [60]	0.0035	0.0034	0.35	0.34
RbCl-20%EG-H_2O [60]	0.0031	0.0031	0.29	0.29
RbCl-30%EG-H_2O [60]	0.0041	0.0041	0.40	0.40
RbCl-40%EG-H_2O [60]	0.0070	0.0069	0.70	0.70
RbCl-10%Glycerol-H_2O [60]	0.0035	0.0035	0.34	0.34
RbCl-20%Glycerol-H_2O [60]	0.0063	0.0063	0.61	0.61
RbCl-30%Glycerol-H_2O [60]	0.0073	0.0073	0.71	0.71
RbCl-40%Glycerol-H_2O [60]	0.0090	0.0090	0.88	0.88
RbF-10%EG-H_2O [61]	0.0011	0.0010	0.10	0.10
RbF-20%EG-H_2O [61]	0.0040	0.0040	0.39	0.39
RbF-30%EG-H_2O [61]	0.0025	0.0019	0.24	0.17
RbF-40%EG-H_2O [61]	0.0040	0.0040	0.36	0.36
RbCl-5%MeOH-5%EtOH-90%H_2O [62]	0.0023	0.0023	0.22	0.22
RbCl-10%MeOH-5%EtOH-85%H_2O [62]	0.0055	0.0055	0.55	0.55
RbCl-5%MeOH-10%EtOH-85%H_2O [62]	0.0054	0.0053	0.54	0.54
RbCl-10%MeOH-10%EtOH-80%H_2O [62]	0.0059	0.0058	0.60	0.60
RbCl-15%MeOH-15%EtOH-70%H_2O [62]	0.0088	0.0088	0.92	0.91
RbF-10%Glycine-H_2O [62]	0.0019	0.0019	0.19	0.19
RbF-20%Glycine-H_2O [62]	0.0048	0.0049	0.48	0.48
RbF-30%Glycine-H_2O [62]	0.0072	0.0073	0.69	0.69
RbF-40%Glycine-H_2O [62]	0.0080	0.0080	0.76	0.76
Average	0.0047	0.0048	0.48	0.48

Figures 1–3 Fitting effects of a single electrolyte containing Rb^+ in different solutions. Figure 1 shows histograms of the relative errors of the fitted activity coefficient and osmotic coefficient of the eMIVM and eMIVM-ET models in aqueous solutions containing Rb^+ single electrolytes. Figure 2 shows line plots of the relative errors of the fitted activity coefficient and osmotic coefficient of the eMIVM and eMIVM-ET models in aqueous solutions containing different concentrations of Rb^+ monoelectrolytes. Figure 3 shows radar plots of the relative error lines of the fitted activity coefficient and osmotic coefficient of the eMIVM and eMIVM-ET models in solutions containing Rb^+ organic electrolytes. From the bar graphs it is clear that most of the orange plots are lower than the blue plots, which shows that the eMIVM model fits better in aqueous electrolyte solutions then. From the line graph, it can be seen that for the same model, the lines with high concentration are completely higher than the lines with low concentration, thus it can be seen that for the same system, the lower the concentration, the better the fitting effect. From the radar plot, it can be seen that the yellow part is basically contained within the red part in the blue background, and the smaller area of the colour block indicates a better fit, thus it

can be seen that the eMIVM-ET model fits better than the eMIVM model in the organic electrolyte solution.

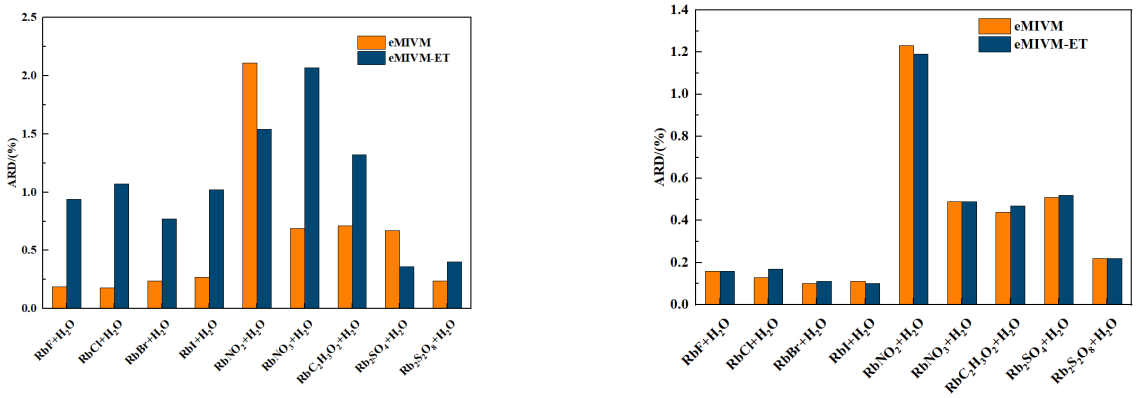

(**a**) (**b**)

Figure 1. (**a**,**b**) show histograms of relative errors in fitting-activity coefficients and osmotic coefficients for the eMIVM and eMIVM-ET models in aqueous solutions containing Rb^+ mono-electrolyte.

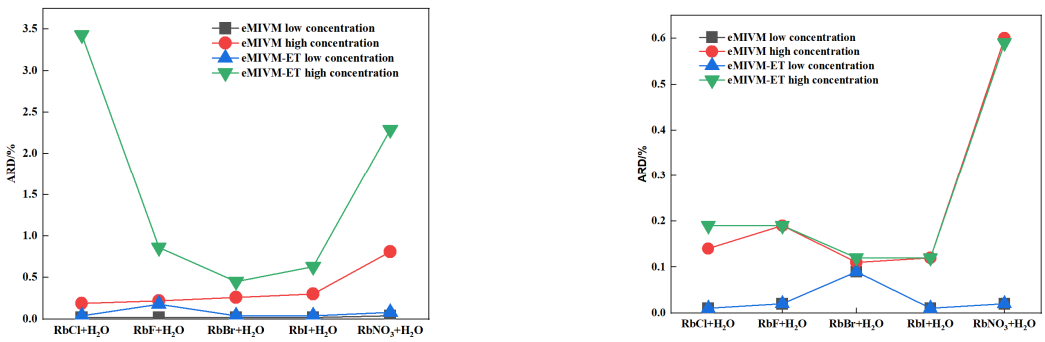

(**a**) (**b**)

Figure 2. (**a**,**b**) show the relative-error-line plots of the fitted-activity coefficients and osmotic coefficients of the eMIVM and eMIVM-ET models in aqueous solutions containing different concentrations of mono-electrolytes of Rb^+.

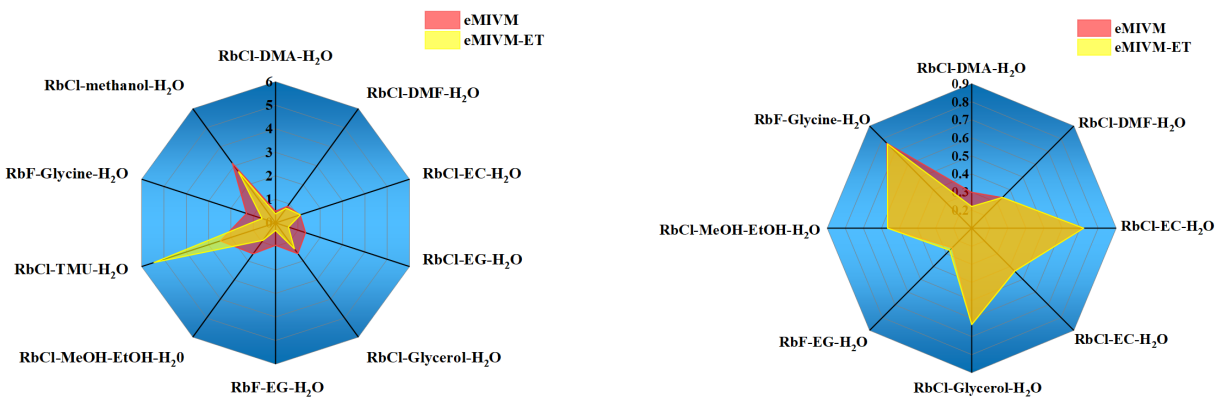

(**a**) (**b**)

Figure 3. (**a**,**b**) show the radar plots of the relative error lines of the fitted-activity coefficients and osmotic coefficients of the eMIVM and eMIVMET models in Rb^+ organic electrolytecontaining solutions.

3.3. Model Predictions

The activity coefficients and osmotic coefficients of the three-component system containing the Rb^+ two-electrolyte solution were predicted based on the basic parameters fitted to the binary system data, which led to further comparisons of the predictive ability of the models. From Table 14, it can be seen that the average standard deviation of the eMIVM-ET model is reduced by 0.0685, and the average relative error is reduced by 11.9% compared to the eMIVM model in the prediction of the activity of the two-electrolyte solutions. As shown in Table 15, the average standard deviation of the eMIVM-ET model was reduced by 0.0348, and the average relative error was reduced by 4.4% compared to the eMIVM model in the prediction of osmotic coefficients of the two-electrolyte solutions. Therefore, the eMIVMET model can be used as a worthy model in predicting the activity coefficients and osmotic coefficients of two-electrolyte solutions.

Table 14. Deviations and relative errors in the prediction of activity coefficient of eMIVM-ET and eMIVM.

System	eMIVM-ET SD	eMIVM SD	eMIVM-ET ARD/%	eMIVM ARD/%
RbF-RbCl-H_2O [65]	0.0539	0.1737	7	23
RbF-RbBr-H_2O [66]	0.0924	0.2042	14	29
RbF-$RbNO_3$-H_2O [66]	0.1313	0.2245	25	40
RbF-Rb_2SO_4-H_2O [67]	0.1203	0.1922	27	39
RbCl-Rb_2SO_4-CH_3OH-H_2O [68]	0.1148	0.1387	34	38
RbCl-Rb_2SO_4-H_2O [69]	0.1091	0.1423	37	51
RbCl-$RbNO_3$-H_2O [70]	0.0626	0.0883	14	18
Average	0.0978	0.1663	23	34

Figures 4 and 5 show relative error plots of the eMIVM and eMIVM-ET model fitted to activity coefficient and osmotic coefficient in two electrolyte solutions containing Rb^+. It is clear from Figure 4 that the yellow plots are closer to the blue plots compared to the red plots, using the blue plots as a standard, which indicates that the eMIVM-ET model is closer to the experimental data. Figure 5 clearly shows that the red plots are closer to the blue plots than the black plots using the blue plots as the standard, which indicates that the eMIVM-ET model is closer to the experimental data. It can be seen that in the prediction of the activity coefficient and osmotic coefficient of the two electrolyte solutions, the eMIVM-ET model is better than the eMIVM model.

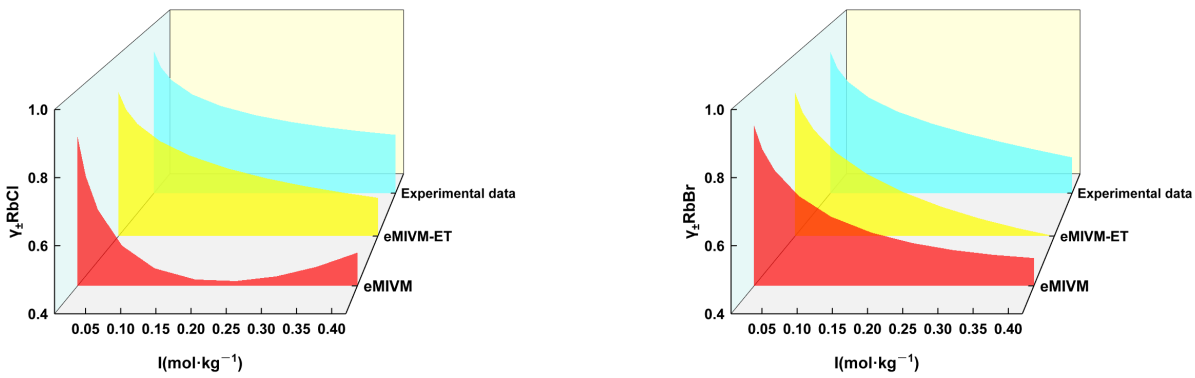

(**a**) (**b**)

Figure 4. *Cont.*

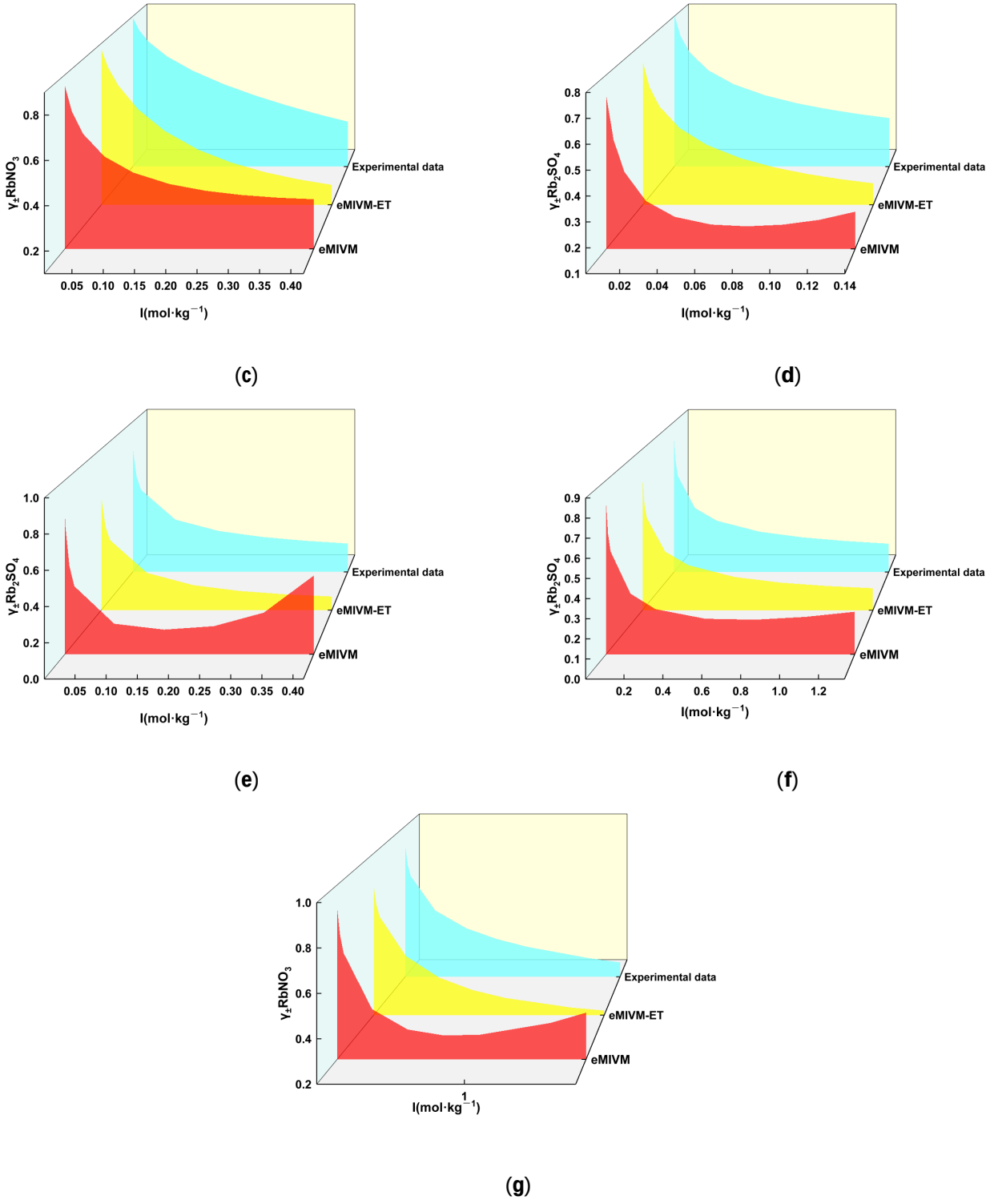

Figure 4. (**a**–**g**) show the RbF-RbCl-H_2O system, RbF-RbBr-H_2O system, RbF-$RbNO_3$-H_2O system, RbF-Rb_2SO_4-H_2O system, RbCl-Rb_2SO_4-CH_3OH-H_2O system, RbCl-Rb_2SO_4-H_2O and RbCl-$RbNO_3$-H_2O system, respectively. Relative error plots for activity-coefficient fitting are shown.

Table 15. Deviations and relative errors in the prediction of osmotic coefficient of eMIVM-ET and eMIVM.

System	eMIVM-ET SD	eMIVM SD	eMIVM-ET ARD/%	eMIVM ARD/%
RbF-RbCl-H_2O [65]	0.0428	0.0833	4	8
RbF-RbBr-H_2O [66]	0.0393	0.2050	3	21
RbF-$RbNO_3$-H_2O [66]	0.1887	0.2757	27	39
RbF-Rb_2SO_4-H_2O [67]	0.0802	0.1269	9	14
RbCl-Rb_2SO_4-CH_3OH-H_2O [68]	0.1364	0.1478	14	16
RbCl-Rb_2SO_4-H_2O [69]	0.1816	0.1500	22	18
RbCl-$RbNO_3$-H_2O [70]	0.1381	0.0620	12	6
Average	0.1153	0.1501	13	17

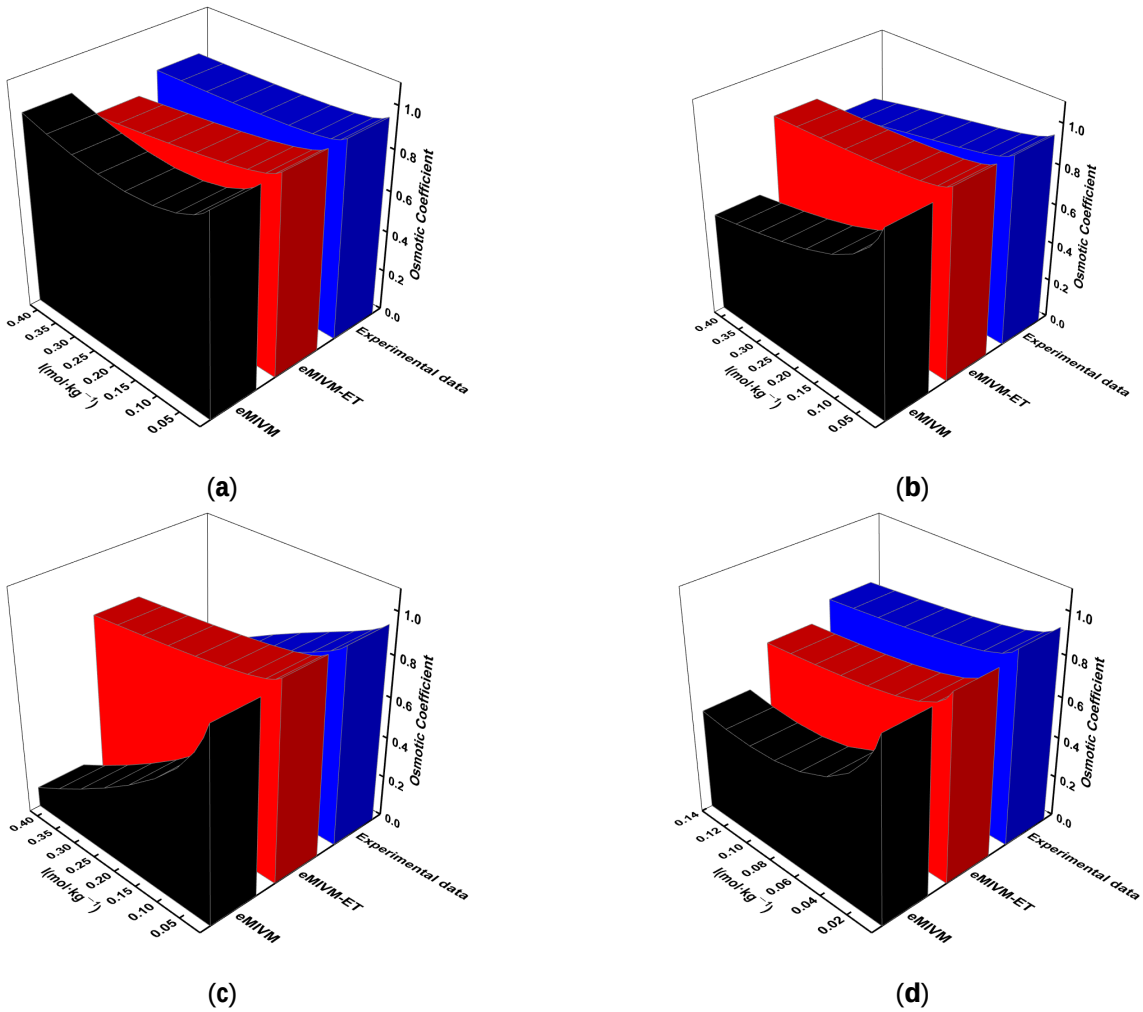

Figure 5. *Cont.*

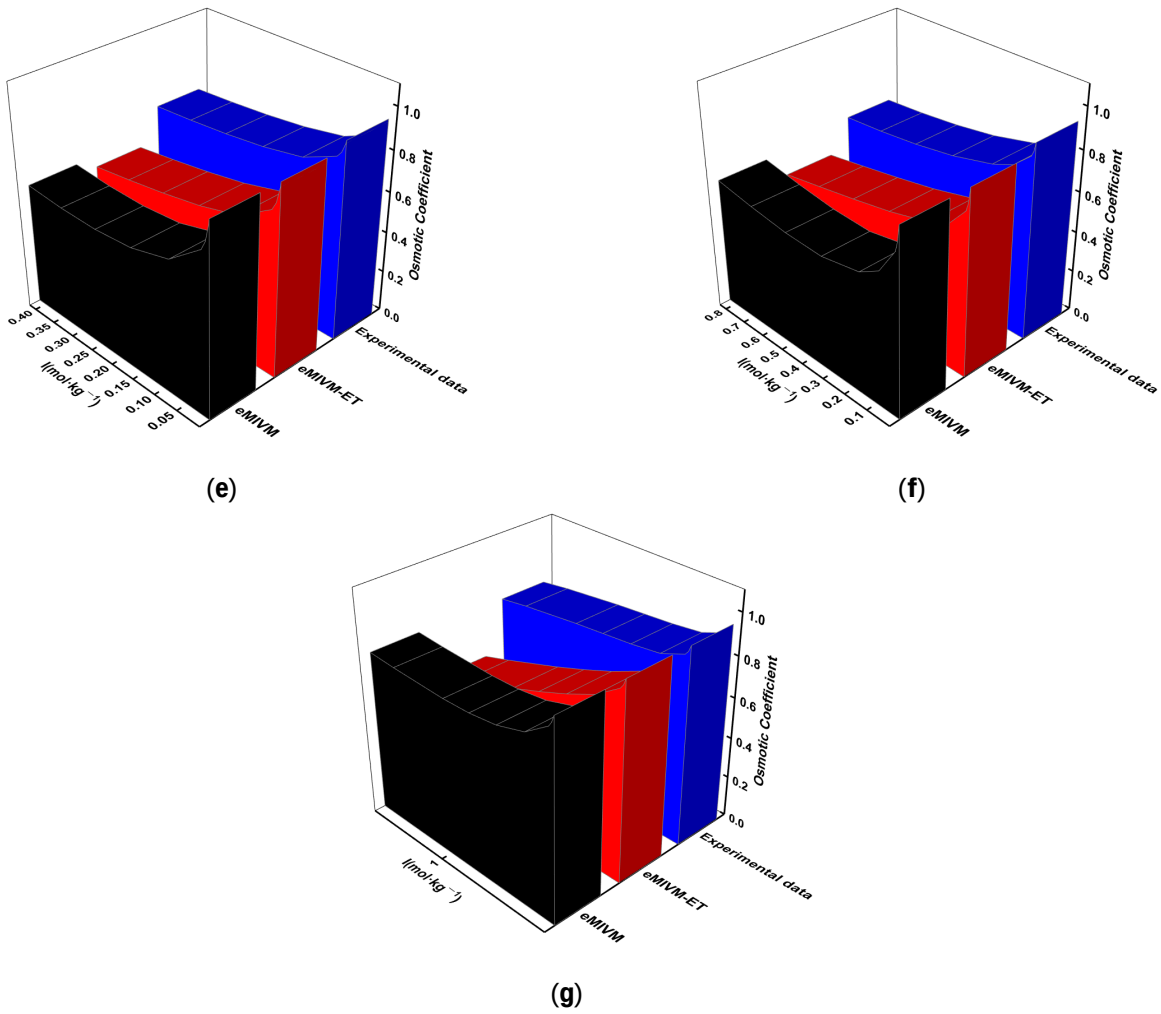

Figure 5. (**a**–**g**) show the RbF-RbCl-H_2O system, RbF-RbBr-H_2O system, RbF-$RbNO_3$-H_2O system, RbF-Rb_2SO_4-H_2O system, RbCl-Rb_2SO_4-CH_3OH-H_2O system, RbCl-Rb_2SO_4-H_2O and RbCl-$RbNO_3$-H_2O system, respectively. Relative error plots for osmotic coefficient fitting are shown.

4. Conclusions

1. In fitting activity and osmotic coefficients to single-electrolyte solutions containing Rb^+, the eMIVM-ET model outperforms the eMIVM model in organic electrolyte solutions. In contrast, the eMIVM model fits better in aqueous electrolyte solutions.
2. In the case of the monoelectrolyte solution of Rb^+, there is minimal variation in the results of binary parameter fitting for the same system at different temperatures. This suggests that the accuracy of predictions remains unaffected by temperature.
3. In the fitting of activity coefficients and osmotic coefficients of electrolyte solutions for the same system, the average deviation and the average relative error are more minor in low-concentration solutions than in high-concentration solutions; i.e., the lower the concentration, the better the fit.
4. In predicting activity coefficients and osmotic coefficients of two-electrolyte solutions, the prediction of the eMIVM-ET model is better than that of the eMIVM model. These calculations can provide alternative models for the future prediction of the thermodynamics of multi-component systems for better guidance for industrial production.

Author Contributions: Conceptualization, D.T.; methodology, Y.W.; software, Y.W.; resources, D.T.; writing—original draft, Y.W.; writing—review and editing, Y.W.; supervision, D.T.; funding acquisition, D.T. All authors have read and agreed to the published version of the manuscript.

Funding: This work is financially supported by the National Natural Science Foundation of China (Grant No. 51464022).

Data Availability Statement: The original contributions presented in the study are included in the article, further inquiries can be directed to the corresponding author.

Acknowledgments: We would like to thank Tianqi He for her participation in the writing and editing of the article, and Chenchen Xu and Shijie Zheng for their contributions to the survey.

Conflicts of Interest: The authors declare no conflict of interest.

References

1. Ramkrishna, D.; Braatz, R.D. Whither chemical engineering? *AIChE J.* **2022**, *68*, e17829. [CrossRef]
2. Horio, M.; Clift, R. Chemical engineering for the Anthropocene. *Can. J. Chem. Eng.* **2023**, *101*, 295–308. [CrossRef]
3. Chagnes, A. Advances in Hydrometallurgy. *Metals* **2019**, *9*, 211. [CrossRef]
4. Han, K.N.; Kim, R.; Kim, J. Recent Advancements in Hydrometallurgy: Solubility and Separation. *Trans. Indian Inst. Met.* **2023**, 1–13. [CrossRef]
5. Li, Z.; Liu, H. Study on electrochemical properties of lead calcium tin anode for hydrometallurgy. *Alex. Eng. J.* **2023**, *82*, 389–395. [CrossRef]
6. Ding, T.; Zheng, M.; Nie, Z.; Ma, L.; Ye, C.; Wu, Q.; Zhao, Y.; Yang, D.; Wang, K. Impact of Regional Climate Change on the Development of Lithium Resources in Zabuye Salt Lake, Tibet. *Front. Earth Sci.* **2022**. [CrossRef]
7. Bekri, E.S.; Kokkoris, I.P.; Christodoulou, C.S.; Sophocleous-Lemonari, A.; Dimopoulos, P. Management Implications at a Protected, Peri-Urban, Salt Lake Ecosystem: The Case of Larnaca's Salt Lakes (Cyprus). *Land* **2023**, *12*, 1781. [CrossRef]
8. Italiano, F.; Solecki, A.; Martinelli, G.; Wang, Y.; Zheng, G. New Applications in Gas Geochemistry. *Geofluids* **2020**, *2020*, 4976190. [CrossRef]
9. Fernandez-Suarez, J.; Sanchez Martinez, S.; Fuenlabrada, J.M. Geochemistry in earth sciences: A brief overview. *J. Iber. Geol.* **2021**, *47*, 3–13. [CrossRef]
10. Deng, H.; Li, L.; Kim, J.J.; Ling, F.T.; Beckingham, L.E.; Wammer, K.H. Bridging environmental geochemistry and hydrology. *J. Hydrol.* **2022**, *613*, 128448. [CrossRef]
11. Franikovi-Bilinski, S.; Sakan, S. Geochemistry of Water and Sediment. *Water* **2021**, *13*, 693. [CrossRef]
12. Lu, B.; Ru, N.; Duan, J.; Li, Z.; Qu, J. In-Plane Porous Graphene: A Promising Anode Material with High Ion Mobility and Energy Storage for Rubidium-Ion Batteries. *ACS Omega* **2023**. [CrossRef]
13. Smith, J.P.; Boyd, T.J.; Cragan, J.; Ward, M.C. Dissolved rubidium to strontium ratio as a conservative tracer for wastewater effluent-sourced contaminant inputs near a major urban wastewater treatment plant. *Water Res.* **2021**, *205*, 117691. [CrossRef] [PubMed]
14. Lau, S.; Atakan, B. Combined Thermogravimetric Determination of Activity Coefficients and Binary Diffusion Coefficients—A New Approach Applied to Ferrocene/n-Tetracosane Mixtures. *J. Chem. Eng. Data* **2019**, *65*, 1211–1221. [CrossRef]
15. Noguchi, D.; Takeda, O.; Abe, T.; Zhu, H.; Sugimoto, S. Determination of activity of RE (RE = Nd and Dy) in molten RE-Fe-B alloys by the electromotive force method. *Thermochim. Acta Int. J. Concerned Broader Asp. Thermochem. Its Appl. Chem. Probl.* **2022**, *709*, 179161. [CrossRef]
16. El Fadel, W.; El Hantati, S.; Nour, Z.; Dinane, A.; Samaouali, A.; Messnaoui, B. Experimental Determination of Osmotic Coefficient and Salt Solubility of System NH_4NO_3–$NH_4H_2PO_4$–H_2O and Their Correlation and Prediction with the Pitzer–Simonson–Clegg Model. *Ind. Eng. Chem. Res.* **2023**, *62*, 17986–17996. [CrossRef]
17. Passamonti, F.J.; de Chialvo MR, G.; Chialvo, A.C. Evaluation of the activity coefficients of ternary molecular solutions from osmotic coefficient data. *Fluid Phase Equilibria* **2022**, *559*, 113464. [CrossRef]
18. Zafarani-Moattar, M.T.; Mokhtarpour, M.; Faraji, S. Osmotic Coefficients of Gabapentin Drug in Aqueous Solutions of Deep Eutectic Solvents: Experimental Measurements and Thermodynamic Modeling. *J. Chem. Eng. Data* **2023**, *68*, 1663–1672.
19. McMillan Jr, W.G.; Mayer, J.E. The statistical thermodynamics of multicomponent systems. *J. Chem. Phys.* **1945**, *13*, 276–305. [CrossRef]
20. Pitzer, K.S. Electrolyte theory-improvements since Debye and Hueckel. *Acc. Chem. Res.* **1977**, *10*, 371–377. [CrossRef]
21. Xiao, T.; Zhou, Y. Fast Calculation of Electrostatic Solvation Free Energy in Simple Ionic Fluids Using an Energy-Scaled Debye–Hückel Theory. *J. Phys. Chem. Lett.* **2021**, *12*, 6262–6268. [CrossRef] [PubMed]
22. Pitzer, K.S. Thermodynamics of electrolytes. I. Theoretical basis and general equations. *J. Phys. Chem.* **1973**, *77*, 268–277. [CrossRef]
23. Pitzer, K.S.; Mayorga, G. Thermodynamics of electrolytes. II. Activity and osmotic coefficients for strong electrolytes with one or both ions univalent. *J. Phys. Chem.* **1973**, *7*, 2300–2308. [CrossRef]
24. Pitzer, K.S.; Kim, J.J. Thermodynamics of electrolytes. IV. Activity and osmotic coefficients for mixed electrolytes. *J. Am. Chem. Soc.* **1974**, *96*, 5701–5707. [CrossRef]
25. Das, B. Pitzer ion interaction parameters of single aqueous electrolytes at 25 °C. *J. Solut. Chem.* **2004**, *33*, 33–45. [CrossRef]
26. Sun, L.; Lei, Q.; Peng, B.; Kontogeorgis, G.M.; Liang, X. An analysis of the parameters in the Debye-Hückel theory. *Fluid Phase Equilibria* **2022**, *556*, 113398. [CrossRef]

27. Michelsen, M.L.; Mollerup, J.M. *Thermodynamic Models: Fundamentals & Computational Aspects*; Tie-Line Publications: Holte, Denmark, 2007.
28. Kunz, W. (Ed.) *Specific Ion Effects*; World Scientific: Hackensack, NJ, USA, 2010.
29. Rowland, D.; Königsberger, E.; Hefter, G.; May, P.M. Aqueous electrolyte solution modelling: Some limitations of the Pitzer equations. *Appl. Geochem.* **2015**, *55*, 170–183. [CrossRef]
30. Voigt, W. Chemistry of salts in aqueous solutions: Applications, experiments, and theory. *Pure Appl. Chem.* **2011**, *83*, 1015–1030. [CrossRef]
31. Chen, C.C.; Bokis, C.P.; Mathias, P. Segment-based excess Gibbs energy model for aqueous organic electrolytes. *AIChE J.* **2001**, *47*, 2593–2602. [CrossRef]
32. Chen, C.; Britt, H.I.; Boston, J.F.; Evans, L.B. Local composition model for excess Gibbs energy of electrolyte systems. Part I: Single solvent, single completely dissociated electrolyte systems. *AIChE J.* **1982**, *28*, 588–596. [CrossRef]
33. Chen, C.C. Some recent developments in process simulation for reactive chemical systems. *Pure Appl. Chem.* **1987**, *59*, 1177–1188. [CrossRef]
34. Thomsen, K.; Rasmussen, P.; Gani, R. Correlation and prediction of thermal properties and phase behaviour for a class of aqueous electrolyte systems. *Chem. Eng. Sci.* **1996**, *51*, 3675–3683. [CrossRef]
35. Thomsen, K.; Rasmussen, P. Modeling of vapor–liquid–solid equilibrium in gas–aqueous electrolyte systems. *Chem. Eng. Sci.* **1999**, *54*, 1787–1802. [CrossRef]
36. Thomsen, K. Modeling electrolyte solutions with the extended universal quasichemical (UNIQUAC) model. *Pure Appl. Chem.* **2005**, *77*, 531–542. [CrossRef]
37. Wang, P.; Anderko, A.; Young, R.D. A speciation-based model for mixed-solvent electrolyte systems. *Fluid Phase Equilibria* **2002**, *203*, 141–176. [CrossRef]
38. Kosinski, J.J.; Wang, P.; Springer, R.D.; Anderko, A. Modeling acid–base equilibria and phase behavior in mixed-solvent electrolyte systems. *Fluid Phase Equilibria* **2007**, *256*, 34–41. [CrossRef]
39. Jaworski, Z.; Czernuszewicz, M.; Gralla, Ł. A comparative study of thermodynamic electrolyte models applied to the Solvay soda system. *Chem. Process Eng.* **2011**, *32*, 135–154. [CrossRef]
40. Zhang, C.; Xing, Y.; Tao, D. A Two-Parameter Theoretical Model for Predicting the Activity and Osmotic Coefficients of Aqueous Electrolyte Solutions. *J. Solut. Chem.* **2020**, *49*, 659–694. [CrossRef]
41. Pitzer, K.S. Electrolytes. From dilute solutions to fused salts. *J. Am. Chem. Soc.* **1980**, *102*, 2902–2906. [CrossRef]
42. Zheng, S.; Xu, C.; Tao, D.P. Prediction of activity coefficients for Cu^{2+}-containing electrolyte solutions. *Nonferrous Met. Eng.* **2023**, *13*, 59–68.
43. Zheng, S.; Xu, C.; Lu, Y.; Tao, D. Prediction of Thermodynamic Properties of Ni^{2+}, Co^{2+}, Cu^{2+} Electrolyte Solutions by eMIVM-ET. *J. Solut. Chem.* **2023**, *52*, 1273–1288. [CrossRef]
44. Tao, D.P. A new model of thermodynamics of liquid mixtures and its application to liquid alloys. *Thermochim. Acta* **2000**, *363*, 105–113. [CrossRef]
45. Simonson, J.M.; Pitzer, K.S. Thermodynamics of multicomponent, miscible ionic systems: The system lithium nitrate-potassium nitrate-water. *J. Phys. Chem.* **1986**, *90*, 3009–3013. [CrossRef]
46. Tao, D.P. The universal characteristics of a thermodynamic model to conform to the Gibbs-Duhem equation. *Sci. Rep.* **2016**, *6*, 35792. [CrossRef]
47. Marcus, Y. Ionic volumes in solution. *Biophys. Chem.* **2006**, *124*, 200–207. [CrossRef]
48. Haghtalab, A.; Peyvandi, K. Electrolyte-UNIQUAC-NRF model for the correlation of the mean activity coefficient of electrolyte solutions. *Fluid Phase Equilibria* **2009**, *281*, 163–171. [CrossRef]
49. Li, F.; Li, W. *Metallurgy and Thermodynamics of Materials*; Metallurgical Industry Press: Beijing, China, 2012.
50. Marcus, Y. Thermodynamics of solvation of ions. Part 6—The standard partial molar volumes of aqueous ions at 298.15 K. *J. Chem. Soc. Faraday Trans.* **1993**, *89*, 713–718. [CrossRef]
51. Longhi, P.; Mussini, T.; Osimani, C. Standard potentials of the rubidium amalgam electrode, and thermodynamic functions for dilute rubidium amalgams and for aqueous rubidium chloride. *J. Chem. Thermodyn.* **1974**, *6*, 227–235. [CrossRef]
52. Palmer, D.A.; Rard, J.A.; Clegg, S.L. Isopiestic determination of the osmotic and activity coefficients of Rb_2SO_4 (aq) and Cs_2SO_4 (aq) at T = (298.15 and 323.15) K, and representation with an extended ion-interaction (Pitzer) model. *J. Chem. Thermodyn.* **2002**, *34*, 63–102. [CrossRef]
53. Hamer, W.J.; Wu, Y.C. Osmotic Coefficients and Mean Activity Coefficients of Uni-univalent Electrolytes in Water at 25 °C. *J. Phys. Chem. Ref. Data* **1972**, *1*, 1047–1100. [CrossRef]
54. Partanen, J.I. Re-evaluation of the thermodynamic activity quantities in aqueous solutions of silver nitrate, alkali metal fluorides and nitrites, and dihydrogen phosphate, dihydrogen arsenate, and thiocyanate salts with sodium and potassium ions at 25 °C. *J. Chem. Eng. Data* **2011**, *56*, 2044–2062. [CrossRef]
55. Robinson, R.A.; Stokes, R.H. *Electrolyte Solutions*; Courier Corporation: North Chelmsford, MA, USA, 2002.
56. Goldberg, R.N. Evaluated activity and osmotic coefficients for aqueous solutions: Bi-univalent compounds of zinc, cadmium, and ethylene bis (trimethylammonium) chloride and iodide. *J. Phys. Chem. Ref. Data* **1981**, *10*, 1–56. [CrossRef]
57. Lu, J.; Li, S.N.; Zhai, Q.; Jiang, Y.; Hu, M. Investigating thermodynamic properties of the ternary systems of MCl (M = K, Rb, Cs) with aqueous mixed solvent: N, N-dimethylacetamide. *J. Mol. Liq.* **2013**, *178*, 15–19. [CrossRef]

58. Wang, L.; Li, S.; Zhai, Q.; Zhang, H.; Jiang, Y.; Zhang, W.; Hu, M. Thermodynamic Study of RbCl or CsCl in the Mixed Solvent DMF + H_2O by Potentiometric Measurements at 298.15 K. *J. Chem. Eng. Data* **2010**, *55*, 4699–4703. [CrossRef]
59. Hao, X.; Li, S.; Zhai, Q.; Jiang, Y.; Hu, M. Phase equilibrium and activity coefficients in ternary systems at 298.15 K: RbCl/CsCl + ethylene carbonate + water. *J. Chem. Thermodyn.* **2016**, *98*, 309–316. [CrossRef]
60. Tang, J.; Ma, Y.; Li, S.; Zhai, Q.; Jiang, Y.; Hu, M. Activity Coefficients of RbCl in Ethylene Glycol + Water and Glycerol + Water Mixed Solvents at 298.15 K. *J. Chem. Eng. Data* **2011**, *56*, 2356–2361. [CrossRef]
61. Wang, L.; Li, S.; Zhai, Q.; Jiang, Y.; Hu, M. Activity Coefficients of RbF or CsF in the Ethene Glycol + Water System by Potentiometric Measurements at 298.15 K. *J. Chem. Eng. Data* **2011**, *56*, 4416–4421. [CrossRef]
62. Du, Y.; Li, S.N.; Zhai, Q.; Jiang, Y.; Hu, M. Activity coefficients in quaternary systems at 298.15 K: RbCl + MeOH + EtOH + H_2O and CsCl + MeOH + EtOH + H_2O systems. *J. Chem. Eng. Data* **2013**, *58*, 2545–2551. [CrossRef]
63. Cao, X.; Chang, Y.; Li, S.; Zhai, Q.; Jiang, Y.; Hu, M. Thermodynamic properties of MCl (M = Na, K, Rb, Cs) + tetramethylurea + water ternary system at 298.2 K. *J. Mol. Liq.* **2020**, *297*, 111924. [CrossRef]
64. Cui, R.F.; Hu, M.C.; Jin, L.H.; Li, S.N.; Jiang, Y.C.; Xia, S.P. Activity coefficients of rubidium chloride and cesium chloride in methanol–water mixtures and a comparative study of Pitzer and Pitzer–Simonson–Clegg models (298.15 K). *Fluid Phase Equilibria* **2007**, *251*, 137–144. [CrossRef]
65. Huang, X.; Li, S.N.; Zhai, Q.; Jiang, Y.; Hu, M. Thermodynamic studies of (RbF + RbCl + H_2O) and (CsF + CsCl + H_2O) ternary systems from potentiometric measurements at T = 298.2 K. *J. Chem. Thermodyn.* **2016**, *103*, 157–164. [CrossRef]
66. Huang, X.; Li, S.N.; Zhai, Q.; Jiang, Y.; Hu, M. Activity Coefficients of RbF in the RbF + RbBr + H_2O and RbF + $RbNO_3$ + H_2O Ternary Systems Using the Potentiometric Method at 298.2 K. *J. Chem. Eng. Data* **2016**, *61*, 3481–3487. [CrossRef]
67. Huang, X.; Li, S.N.; Zhai, Q.; Jiang, Y.; Hu, M. Thermodynamic investigation of RbF + Rb_2SO_4 + H_2O and CsF + Cs_2SO_4 + H_2O ternary systems by potentiometric method at 298.2 K. *Fluid Phase Equilibria* **2017**, *433*, 31–39. [CrossRef]
68. Shi-Yang, G.; Shu-Ping, X. Study of thermodynamic properties of quaternary mixture RbCl + Rb_2SO_4 + CH_3OH + H_2O by EMF measurement at 298.15 K. *Fluid Phase Equilibria* **2004**, *226*, 307–312.
69. Shi-Yang, G.; Shu-Ping, X. Determination of thermodynamic properties of aqueous mixtures of RbCl and Rb_2SO_4 by the EMF method at T = 298.15 K. *J. Chem. Thermodyn.* **2003**, *35*, 1383–1392.
70. Xia, S.P. Experimental determination and prediction of activity coefficients of RbCl in aqueous (RbCl + $RbNO_3$) mixture at T = 298.15 K. *J. Chem. Thermodyn.* **2005**, *37*, 1162–1167.